Electronic Supplementary Material (ESI) for ChemComm.

Supporting Information

Intramolecular Frustrated Lewis Pair Mediated Approach to the C=O Bond Activation and Cleavage of Carbon Dioxide

Chamila P. Manankandayalage, Nanda Kumar Katakam, Daniel K. Unruh, Clemens Krempner

Texas Tech University, Department of Chemistry & Biochemistry, Box 41061, Lubbock, Texas, 79409-1061.

Clemens.krempner@ttu.edu

1. General Remarks

All air- and moisture-sensitive manipulations were carried out using standard vacuum line, Schlenk or cannula techniques or in a Vacuum Atmospheres OMNI inert atmosphere dry box containing an atmosphere of purified nitrogen. Toluene, hexanes and benzene were distilled under nitrogen from alkali metals and stored over 4 Å molecular sieves prior to use. All deuterated solvents were purchased from Cambridge Isotope Labs. C_6D_6, CD_2Cl_2, DMSO-d_6 dried and stored over 4 Å molecular sieves prior to use. All the non-sensitive reactions were carried out using the undried solvents. Me_3SiOTf (TCI), MeOTf (Matrix Scientifics), Tf_2O (TCI), Et_3PO (Across Organics) were purchased form commercial sources and used without further purification. Compound **1** [14], $Al(C_6F_5)_3$ [15], $B(C_6F_5)_3$ [16] were prepared according to literature procedures. The ^1H-, ^{13}C-, ^{11}B- ^{19}F-NMR spectra were obtained from a JOEL ECS 400. All measurements, unless noted otherwise, were carried out at 298 K and NMR chemical shifts were given in ppm. The ^{11}B NMR spectra referenced to H_3BO_3 in D_2O (δ = 36 ppm), ^{19}F NMR spectrum was referenced to $C_6H_5CF_3$ in C_6D_6 (δ = 62.3 ppm), The ^1H-NMR spectra were referenced to the residual protonated solvent for ^1H and the ^{13}C NMR spectra were referenced to the deuterated solvent peaks. The following abbreviations were used to describe peak multiplicities in the reported NMR spectroscopic data: “s” for singlet, “d” for doublet, “t” for triplet, “q” for quartet, “sept” for septet, “m” for multiplet and “br” for broadened resonances. Elemental analyses were performed using a Perkin Elmer 2400 Series II CHNS/O Analyzer. The IR spectra were obtained from a Nicolet iS 5 FT-IR spectrometer with iD5 ATR accessory.

2. Experimental

2.1 Synthesis of **2**

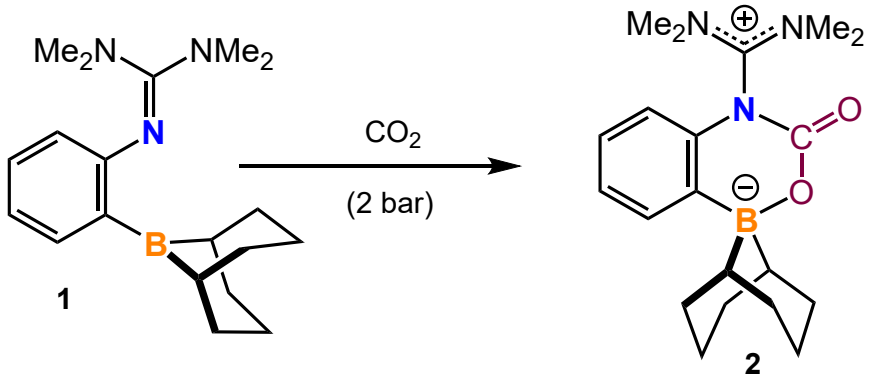

A 40 mL scintillation vial with magnetic stir bar was charged with **1** (0.5 g, 1.6 mmol) and hexanes (10 mL). The vial was placed in a Parr reactor and pressurized with CO_2 (2 bar). After the reaction mixture was stirred for overnight at room temperature, the Parr reactor was vented, and the resulting suspension transferred to a 30 mL Schlenk flask. After centrifugation, the precipitate was washed twice with dry hexanes, once with benzene and subsequently dried under vacuum to give **2** as a colorless solid. Yield 0.53 g (93%). ^{1}H NMR [400 MHz, CD_2Cl_2]: 7.87 (d, $^{3}\boldsymbol{J}_{H\text{-}H}$ = 8 Hz, CH-aryl, 1 H), 7.02-7.10 (m, CH-aryl, 2 H), 6.10 (d, $^{3}\boldsymbol{J}_{H\text{-}H}$ = 8 Hz, CH-aryl, 1 H), 3.21 (s, CH_3, 6 H), 2.96 (s, CH_3, 6 H), 1.89-2.19 (m, CH_2-BBN, 6 H), 1.48-1.71 (m, CH_2-BBN, 6 H), 0.70 (s, CH-BBN, 2 H) ppm. ^{13}C{H} NMR [100.4 MHz, CD_2Cl_2]: 162.0 (C=O), 152.1 (C=N), 147.1 (C-B), 139.8 (C-aryl), 134.2, 125.5, 124.6, 113.5 (CH-aryl), 42.9, 41.1 (CH_3), 32.8, 31.4 (CH_2), 26.6 (CH), 25.5, 25.4 (CH_2) ppm. ^{11}B NMR [128.4 MHz, CD_2Cl_2]: -2.5 ppm. Anal. Calc. for $C_{20}H_{30}BN_3O$ (355.24): C, 67.61; H, 8.51, N, 11.83, Found: C, 67.32; H, 8.64, 11.68. IR (solid) $\tilde{\nu}_{(C=O)}$ = 1707 cm^{-1}; $\tilde{\nu}_{(C=N)}$ = 1628 cm^{-1}.

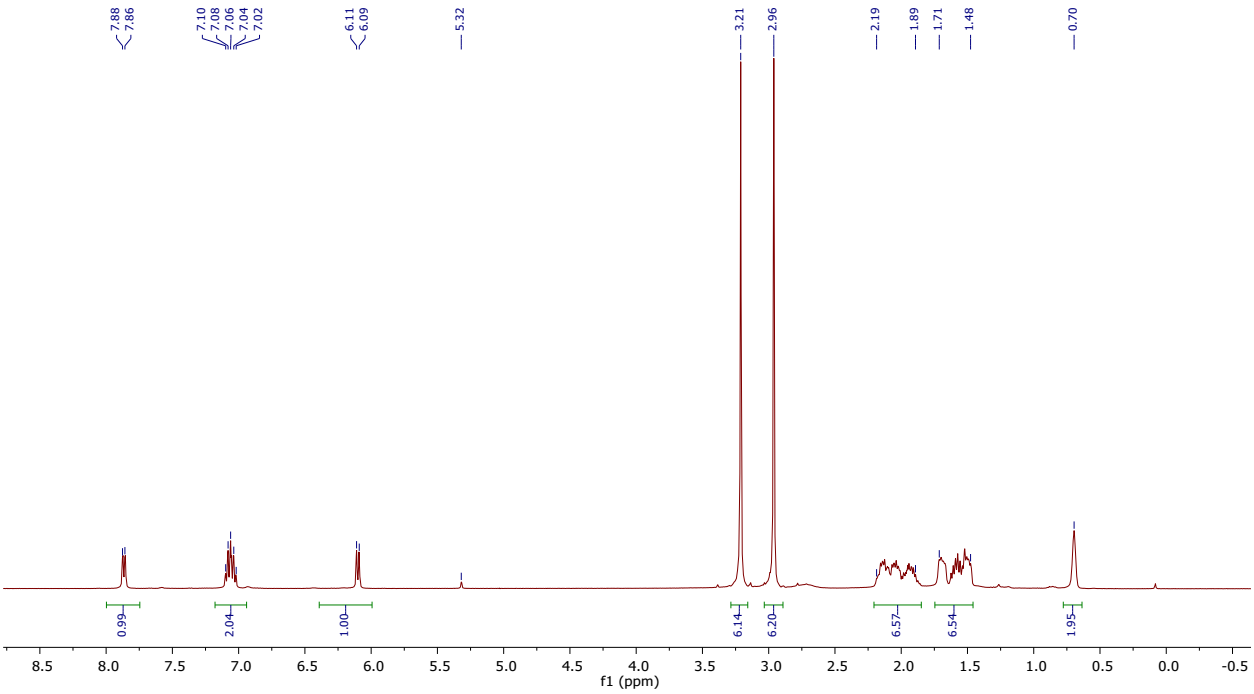

Figure S1. ^{1}H NMR spectrum of **2** in CD_2Cl_2 at room temperature.

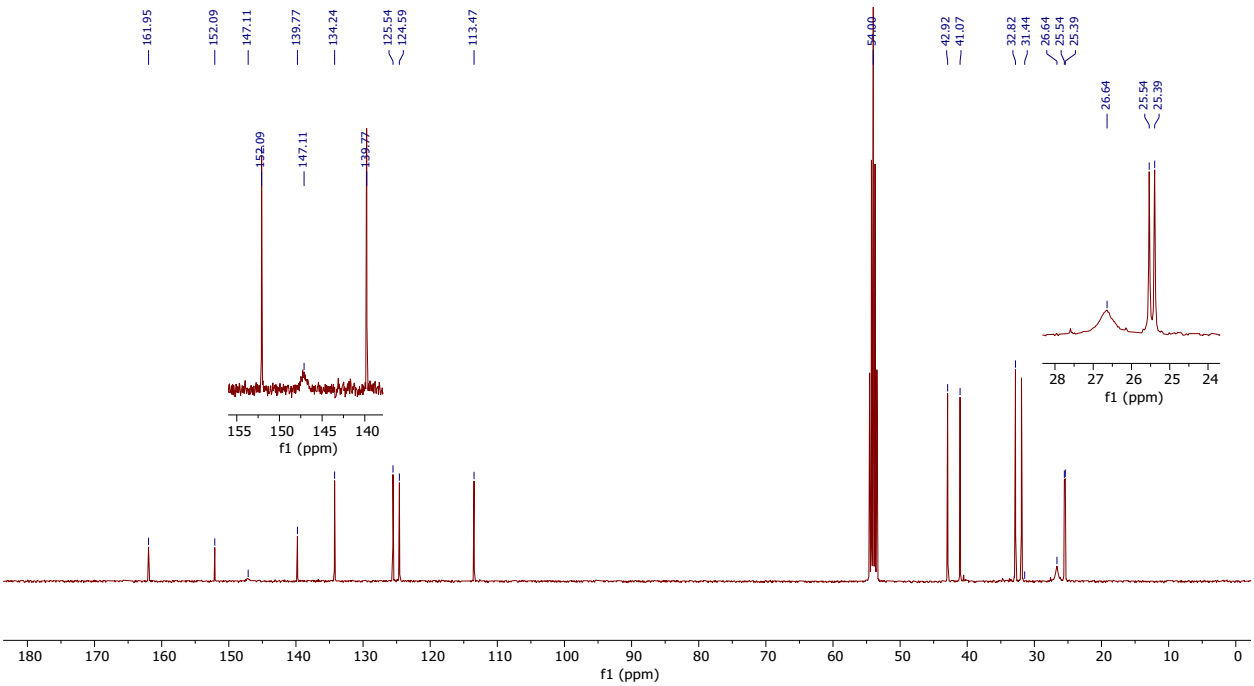

Figure S2. $^{13}C\{H\}$ NMR spectrum of **2** in CD_2Cl_2 at room temperature.

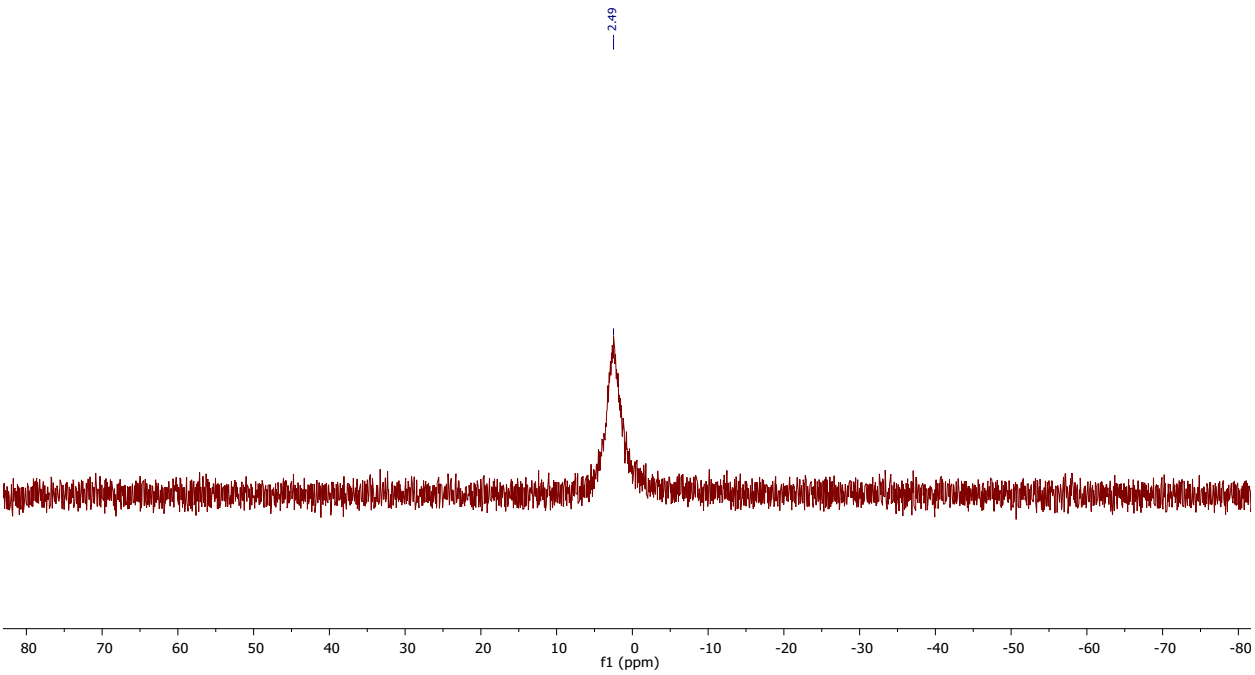

Figure S3. ^{11}B NMR spectrum of **2** in CD_2Cl_2 at room temperature.

2.2 Synthesis of **3**

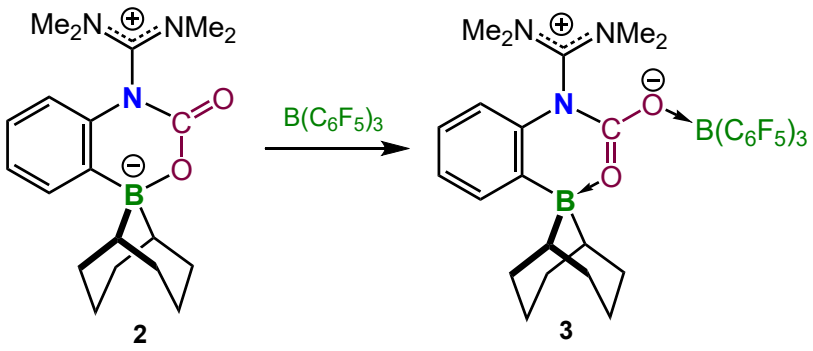

In the glove box, a 30 mL Schlenk flask was charged with **2** (92 mg, 0.26 mmol), $B(C_6F_5)_3$ (133 mg, 0.26 mmol) and CH_2Cl_2 (10 mL). The reaction mixture was stirred for 3 hours at room temperature. The resulting precipitate was centrifuged, washed once with dichloromethane and dried under vacuum to give **3** as a colorless crystalline solid. Yield 180 mg (75 %). ^{1}H NMR [400 MHz, DMSO-d_6]: 7.71 (d, $^{3}J_{H-H}$ = 8 Hz, CH-aryl, 1 H), 7.01-7.08 (m, CH-aryl, 2 H), 6.34 (d, $^{3}J_{H-H}$ = 8 Hz, CH-aryl, 1 H), 3.29 (s, CH_3, 6 H), 2.88 (s, CH_3, 6 H), 1.84-2.19 (m, CH_2-BBN, 6 H), 1.40-1.68 (m, CH_2-BBN, 6 H), 0.68 (s, CH-BBN, 2 H) ppm. ^{13}C{H} NMR [125 MHz, DMSO-d_6]: 158.9 (C=O), 151.1 (C=N), 147.2 (d, $^{1}J_{C-F}$ = 235 Hz, C-F), 144.8 (C-B), 139.3 (C-aryl), 139.1 (d, $^{1}J_{C-F}$ = 235 Hz, C-F), 136.3 (d, $^{1}J_{C-F}$ = 238 Hz, C-F), 132.5, 125.0, 123.3 (CH-aryl), 118.8 (C-quart.) 112.9 (CH-aryl), 41.8, 40.0 (CH_3), 31.9, 30.5 (CH_2), 25.4 (CH), 24.7, 24.5 (CH_2) ppm. ^{19}F NMR [376.3 MHz, DMSO-d_6]: -163.7 (t, $^{3}J_{F-F}$ = 23 Hz), -157.1 (t, $^{3}J_{F-F}$ = 23 Hz), -133.1 (d, $^{3}J_{F-F}$ = 23 Hz) ppm. Anal. Calc. for $C_{38}H_{30}B_2F_{15}N_3O$•1/2$CH_2Cl_2$ (915.21): C, 51.15; H, 3.41, N, 4.59, Found: C, 51.25; H, 3.37, 4.71.

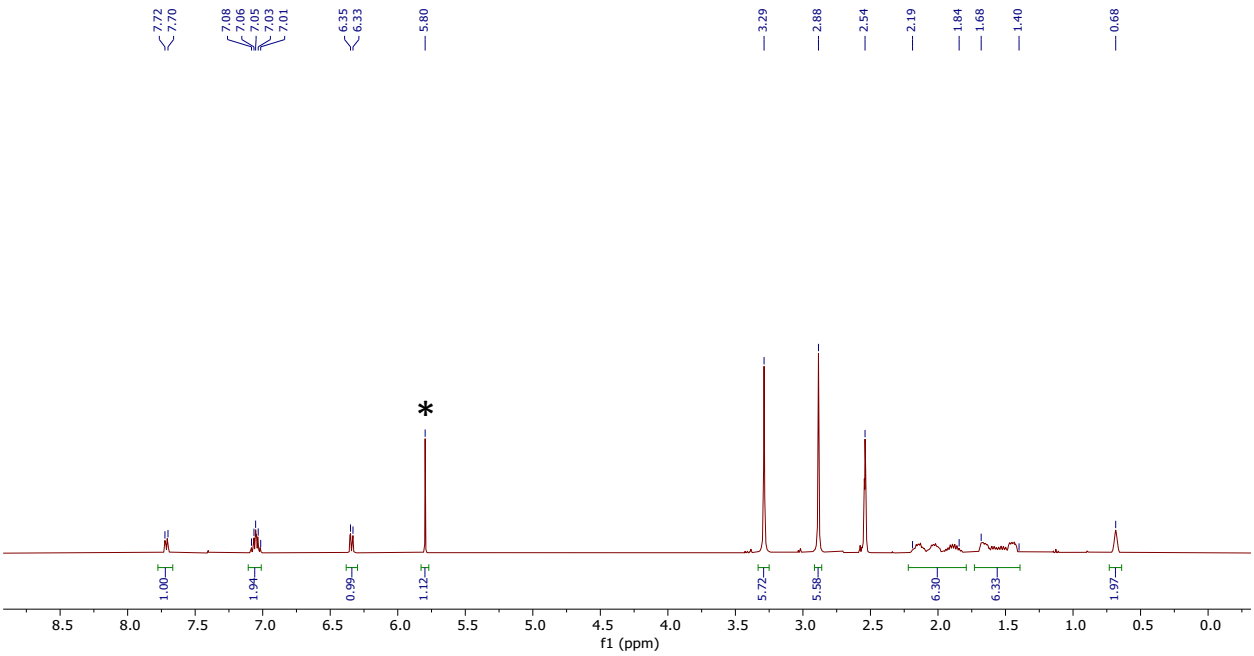

Figure S4. ^{1}H NMR spectrum of **3** in DMSO-d_6 at room temperature (trace amount of CH_2Cl_2 labelled with asterisks).

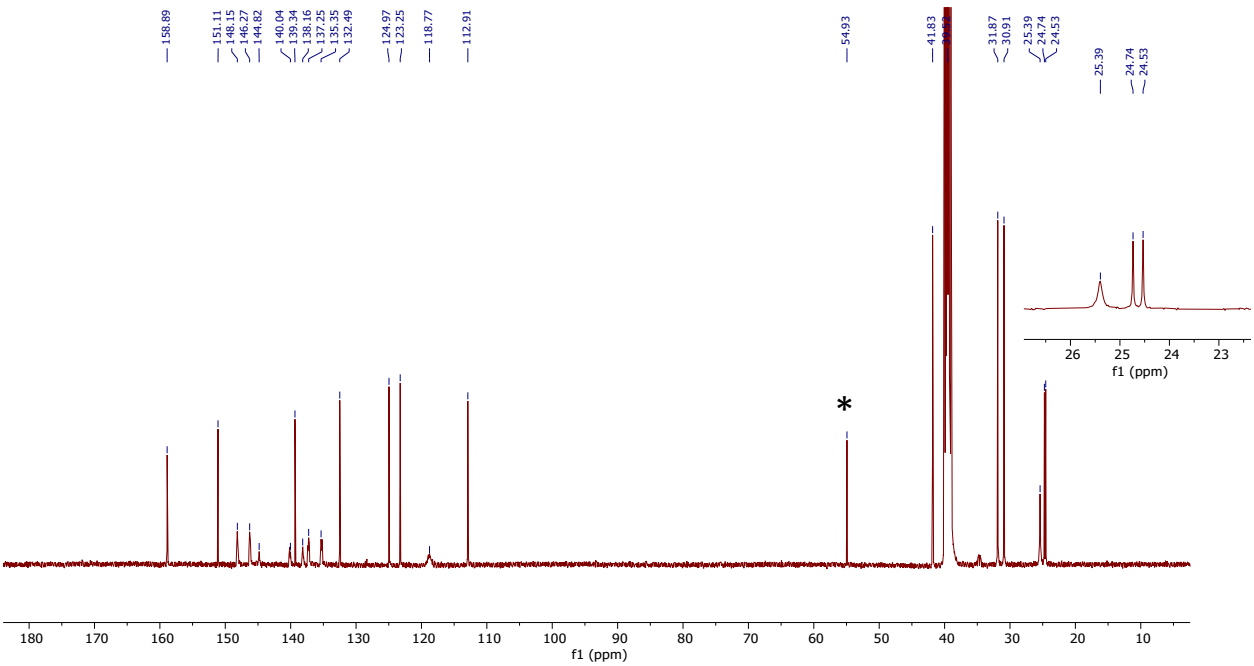

Figure S5. $^{13}C\{H\}$ NMR spectrum of **3** in DMSO-d_6 at room temperature.

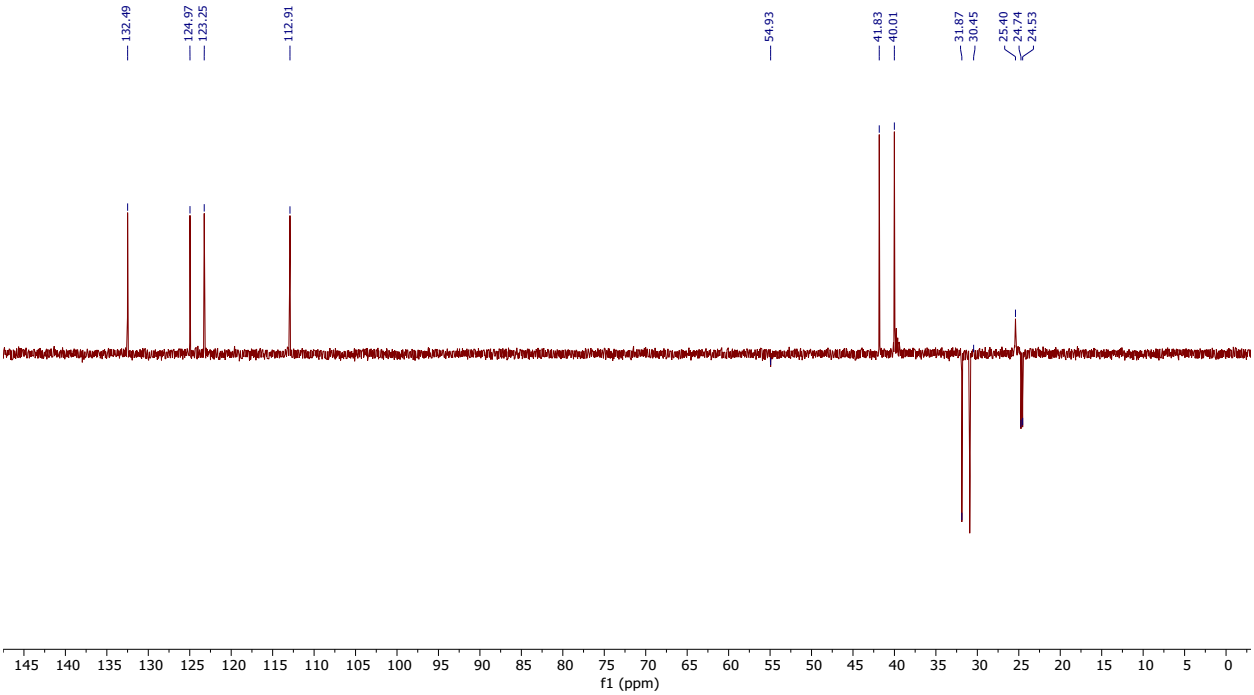

Figure S6. $^{13}C\{H\}$ (DEPT) NMR spectrum of **3** in DMSO-d_6 at room temperature.

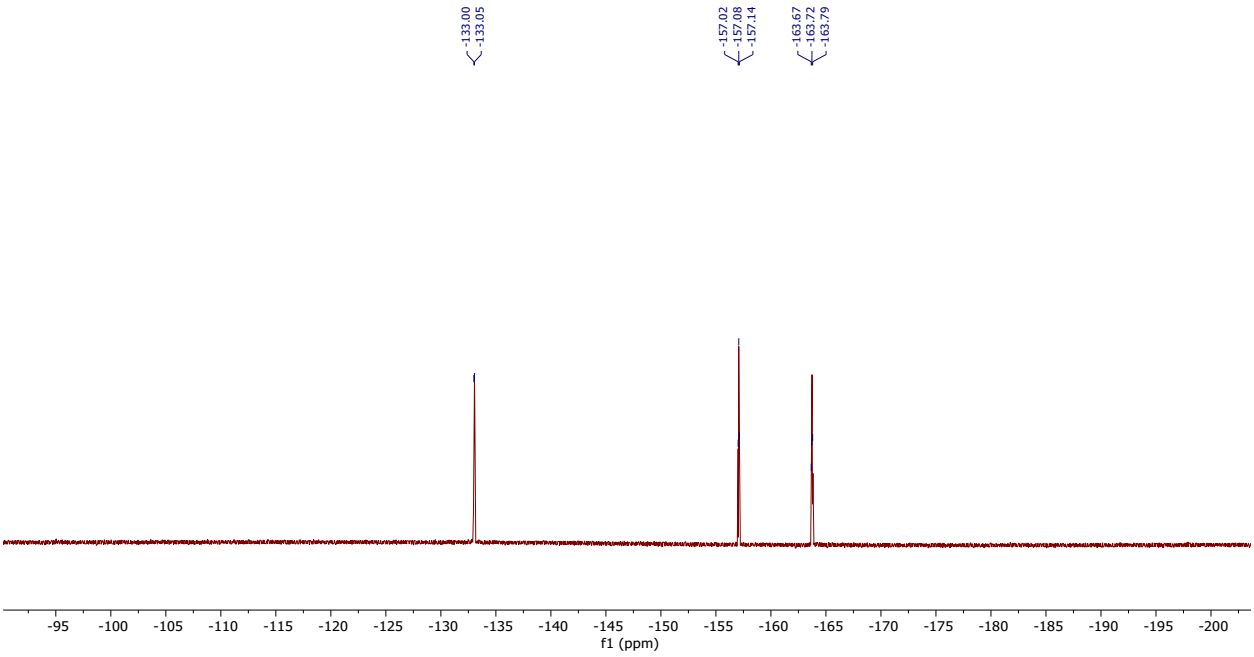

Figure S7. ^{19}F NMR spectrum of **3** in DMSO-d_6 at room temperature.

2.3 Synthesis of **4**

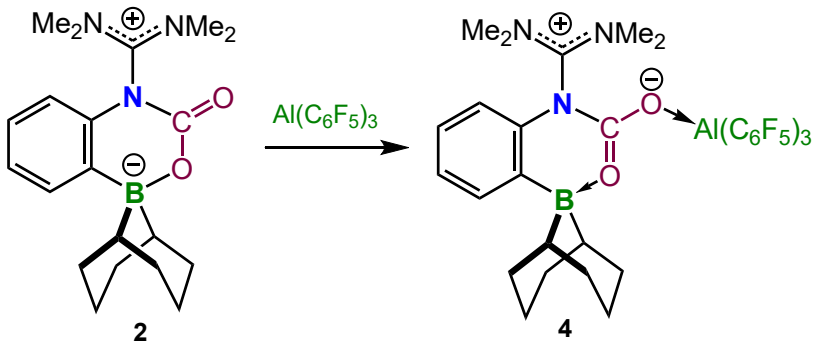

2 **4**

In the glove box, a 30 mL Schlenk flask was charged with **2** (100 mg, 0.28 mmol), $Al(C_6F_5)_3$•1/3toluene (157 mg, 0.28 mmol) and benzene (6 mL). The reaction mixture was stirred for 3 hours at room temperature. The resulting precipitate was centrifuged, washed once with benzene and dried under vacuum to give **4** as a colorless crystalline solid. Yield 200 mg (85%). ^{1}H NMR [400 MHz, CD_2Cl_2]: 7.85 (d, $^{3}J_{H\text{-}H}$ = 8 Hz, CH-aryl, 1 H), 7.22 (t, $^{3}J_{H\text{-}H}$ = 8 Hz, CH-aryl, 1 H), 7.15 (t, $^{3}J_{H\text{-}H}$ = 8 Hz, CH-aryl, 1 H), 6.17 (d, $^{3}J_{H\text{-}H}$ = 8 Hz, CH-aryl, 1 H), 3.32 (s, CH_3, 6 H), 3.14 (s, CH_3, 6 H), 1.05-2.13 (m, CH_2-BBN, 12 H), 0.66 (s, CH-BBN, 2 H) ppm. ^{13}C{H} NMR [125 MHz, CD_2Cl_2]: 158.3 (C=O), 154.5 (C=N), 150.4 (dd, $^{1}J_{C\text{-}F}$ = 229 Hz, $^{2}J_{C\text{-}F}$ = 20 Hz, C-F), 142.3 (C-B), 141.8 (d, $^{1}J_{C\text{-}F}$ = 250 Hz, C-F), 137.4 (d, $^{1}J_{C\text{-}F}$ = 250 Hz, C-F), 135.3 (C-aryl), 135.2 (CH-aryl), 126.6, 126.6 (CH-aryl), 115.4 (C-quart.), 111.9 (CH-aryl), 43.4, 41.7 (CH_3), 31.8, 30.8 (CH_2), 26.6 (CH), 25.0, 24.4 (CH_2) ppm. ^{19}F NMR [376.3 MHz, CD_2Cl_2]: -161.8, -153.4, -123.3 ppm. ^{11}B NMR [128.4 MHz, CD_2Cl_2]: 3.2 ppm. Anal. Calc. for $C_{38}H_{30}AlBF_{15}N_3O$ (867.433): C, 52.62; H, 3.49, N, 4.84, Found: C, 52.18; H, 3.24, 4.55.

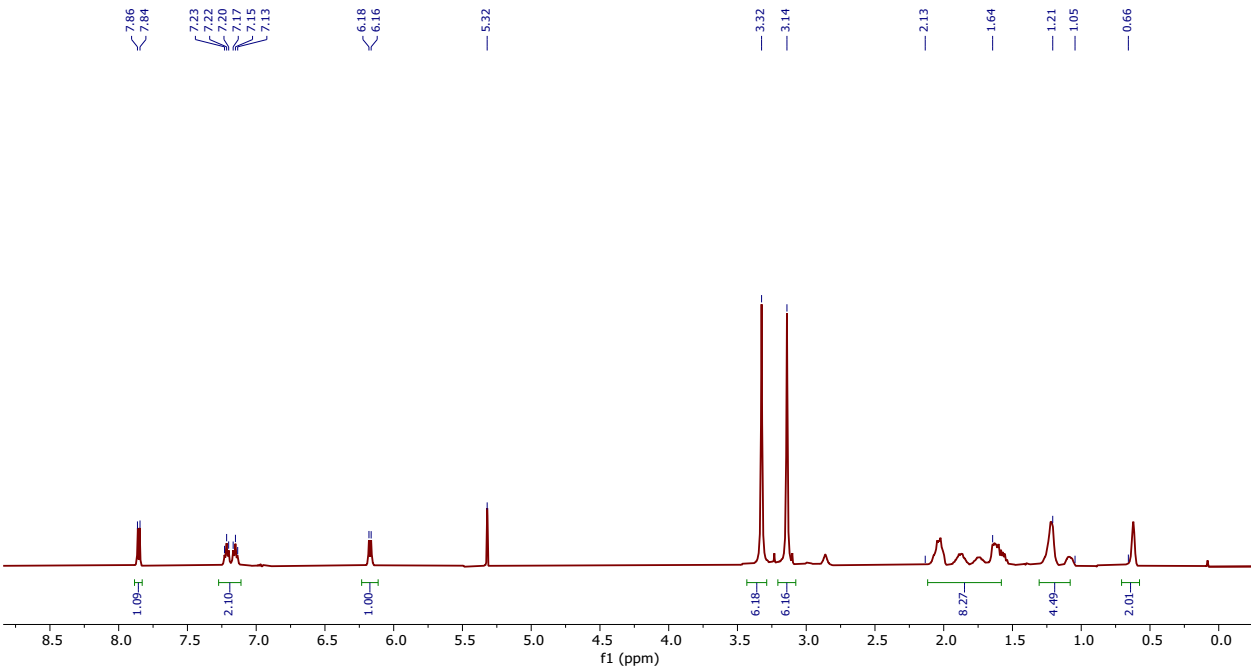

Figure S8. ^{1}H NMR spectrum of **4** in CD_2Cl_2 at room temperature.

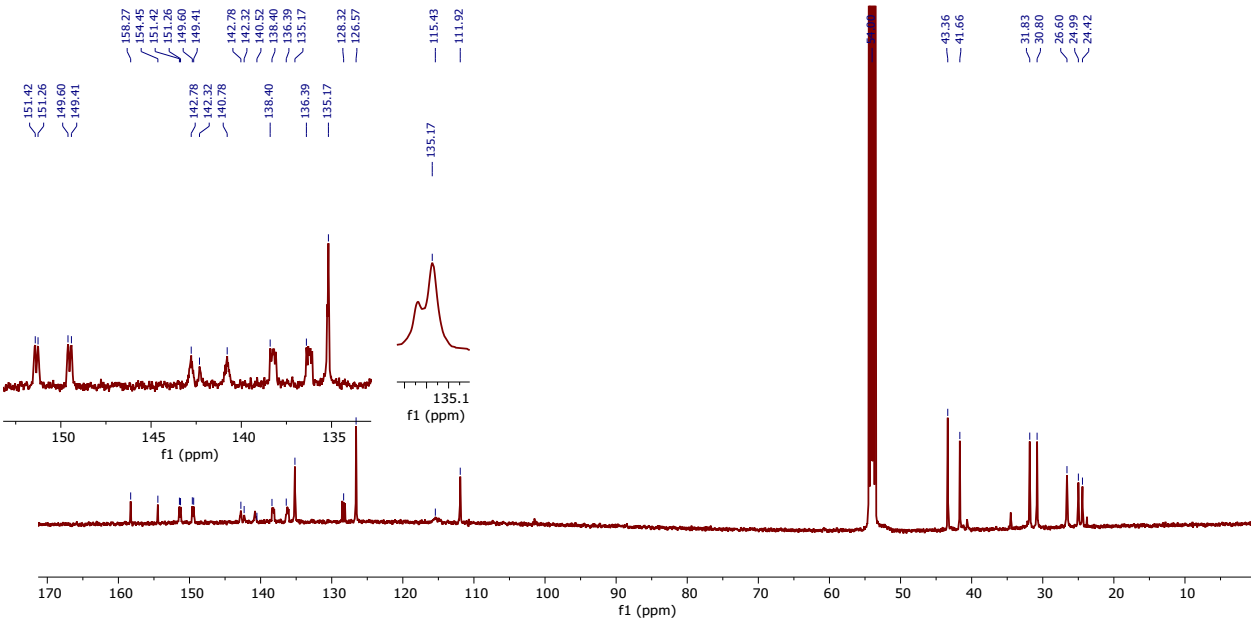

Figure S9. $^{13}C\{H\}$ NMR spectrum of **4** in CD_2Cl_2 at room temperature.

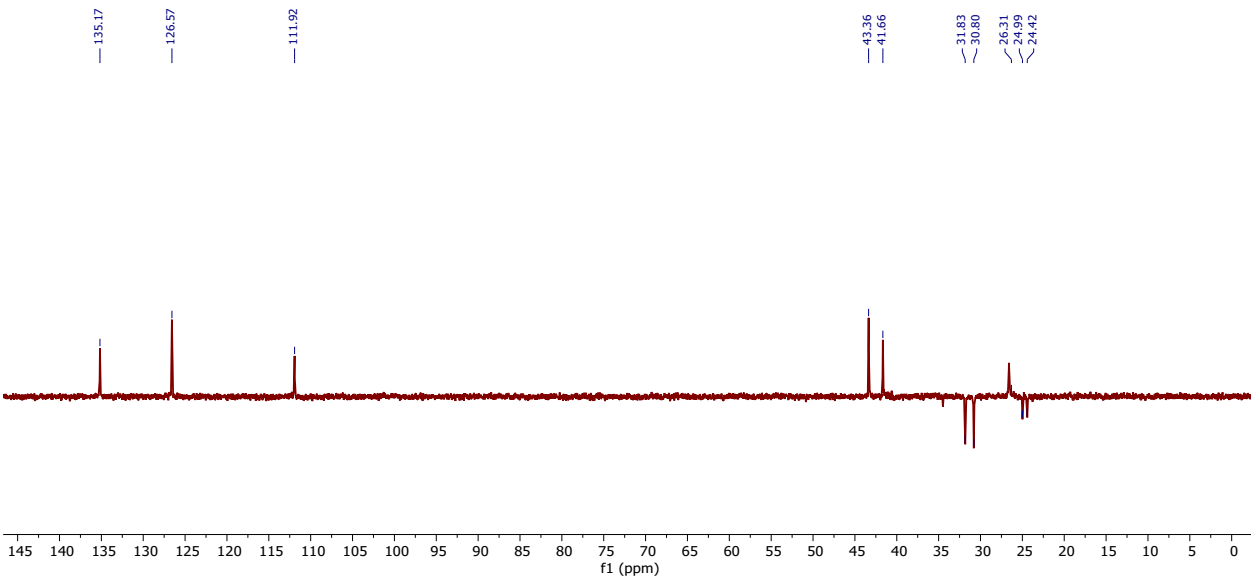

Figure S10. $^{13}C\{H\}$ (DEPT) NMR spectrum of **4** in CD_2Cl_2 at room temperature.

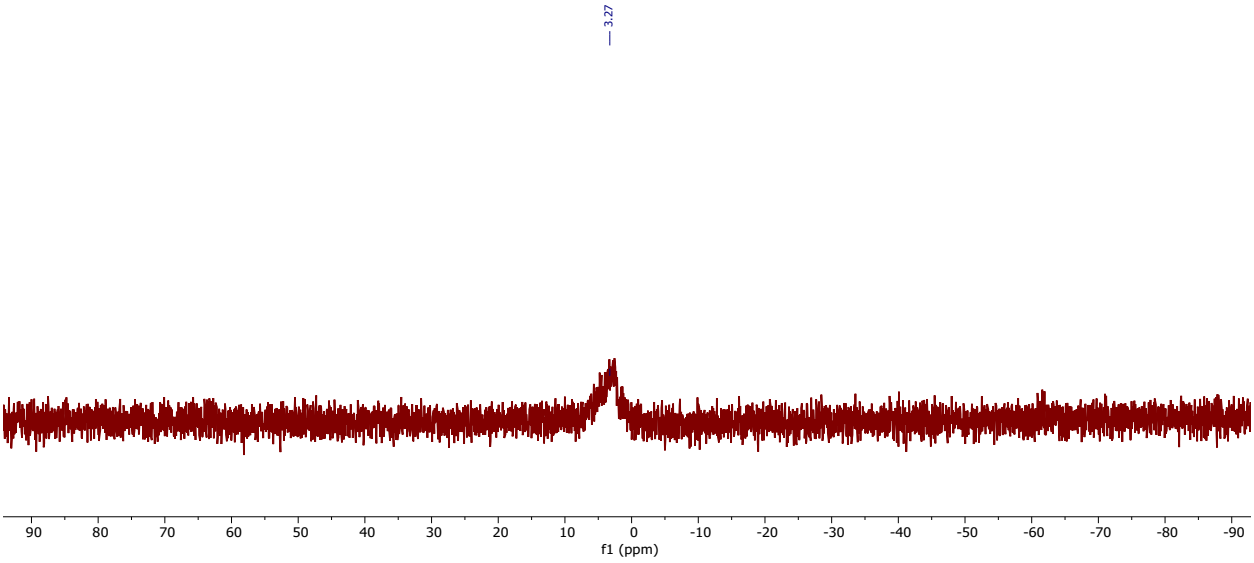

Figure S11. ^{11}B NMR spectrum of **4** in CD_2Cl_2 at room temperature.

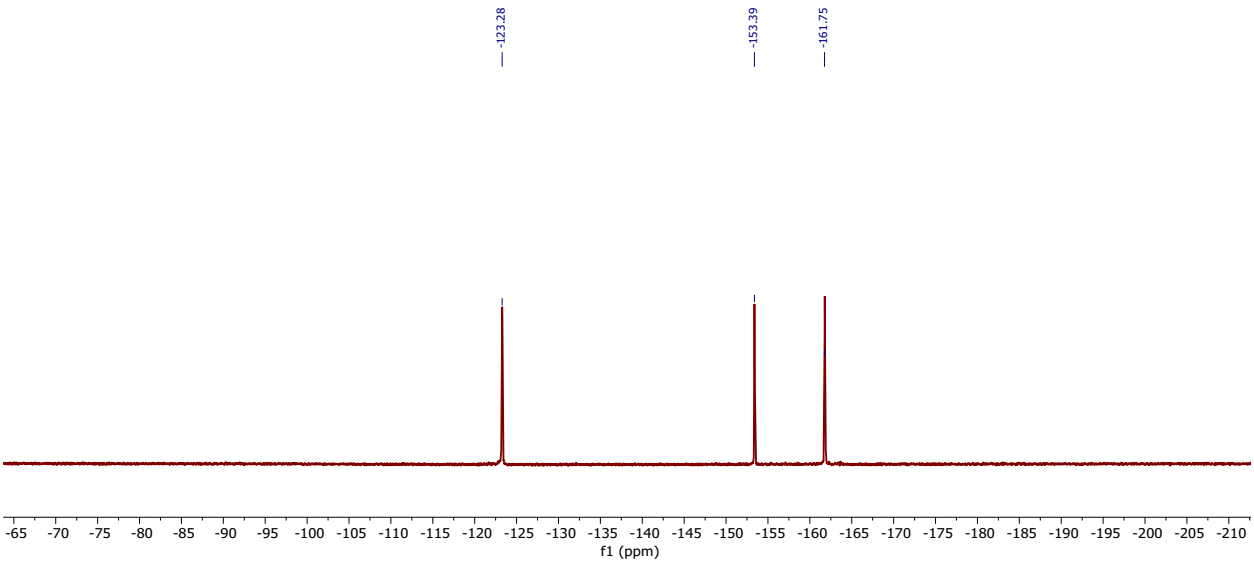

Figure S12. ^{19}F NMR spectrum of **4** in CD_2Cl_2 at room temperature.

2.4 Synthesis of **6**

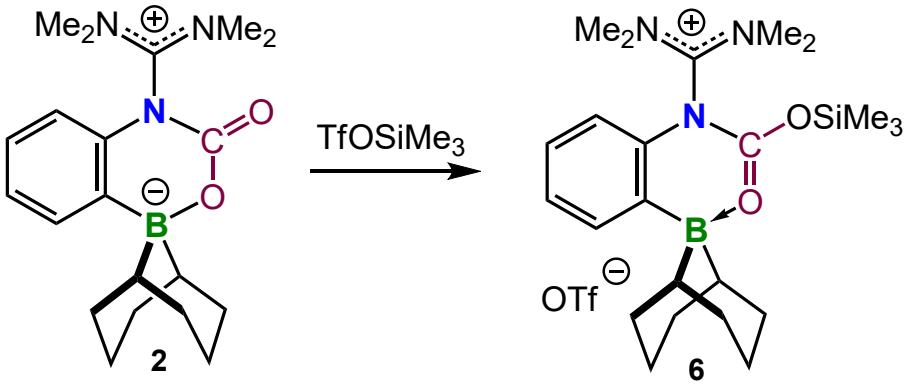

In the glove box, a 30 mL Schlenk flask was charged with **2** (100 mg, 0.28 mmol), Me_3SiOTf (63 mg, 0.28 mmol) and benzene (6 mL). The reaction mixture was stirred for 3 hours at room temperature. The resulting precipitate was centrifuged, washed once with benzene and dried under vacuum to give **6** as a colorless crystalline solid. Yield 130 mg (80%) ^{1}H NMR [400 MHz, C_6D_6]: 8.05 (d, $^{3}J_{H-H}$ = 8 Hz, CH-aryl, 1 H), 7.32 (t, $^{3}J_{H-H}$ = 8 Hz, CH-aryl, 1 H), 7.15-7.18 (m, CH-aryl, 1 H), 6.69 (d, $^{3}J_{H-H}$ = 8 Hz, CH-aryl, 1 H), 3.33 (s, CH_3, 6 H), 2.55 (s, CH_3, 6 H), 1.93-2.37 (m, CH_2-BBN, 12 H), 1.24 (s, CH-BBN, 2 H), 0.33 (s, $SiMe_3$, 9 H) ppm. $^{13}C\{H\}$ NMR [125 MHz, C_6D_6]: 155.2 (C=O), 154.3 (C=N), 141.0 (C-B),135.8 (C-aryl), 134.5, 127.8, 127.7 (CH-aryl),122.0 (q, $^{1}J_{C-F}$ 322 Hz, CF_3), 115.1 (CH-aryl), 43.0, 41.0 (CH_3), 32.4 (CH_2), 26.8 (CH), 25.1 (CH_2), 0.0 ($SiMe_3$) ppm. ^{19}F NMR [376.3 MHz, C_6D_6]: -77.6 ppm. ^{29}Si NMR [99.4 MHz, C_6D_6]: 39.5 ppm. The combustion analysis of the title compound gave unsatisfactory results.

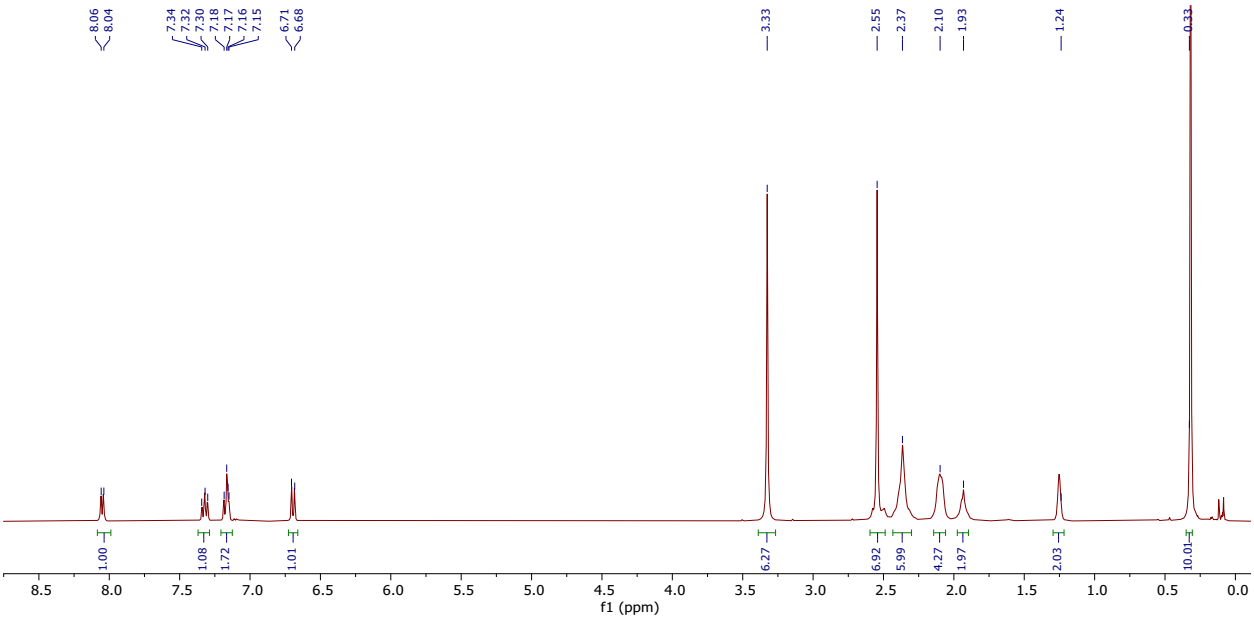

Figure S13. ^{1}H NMR spectrum of **6** in C_6D_6 at room temperature.

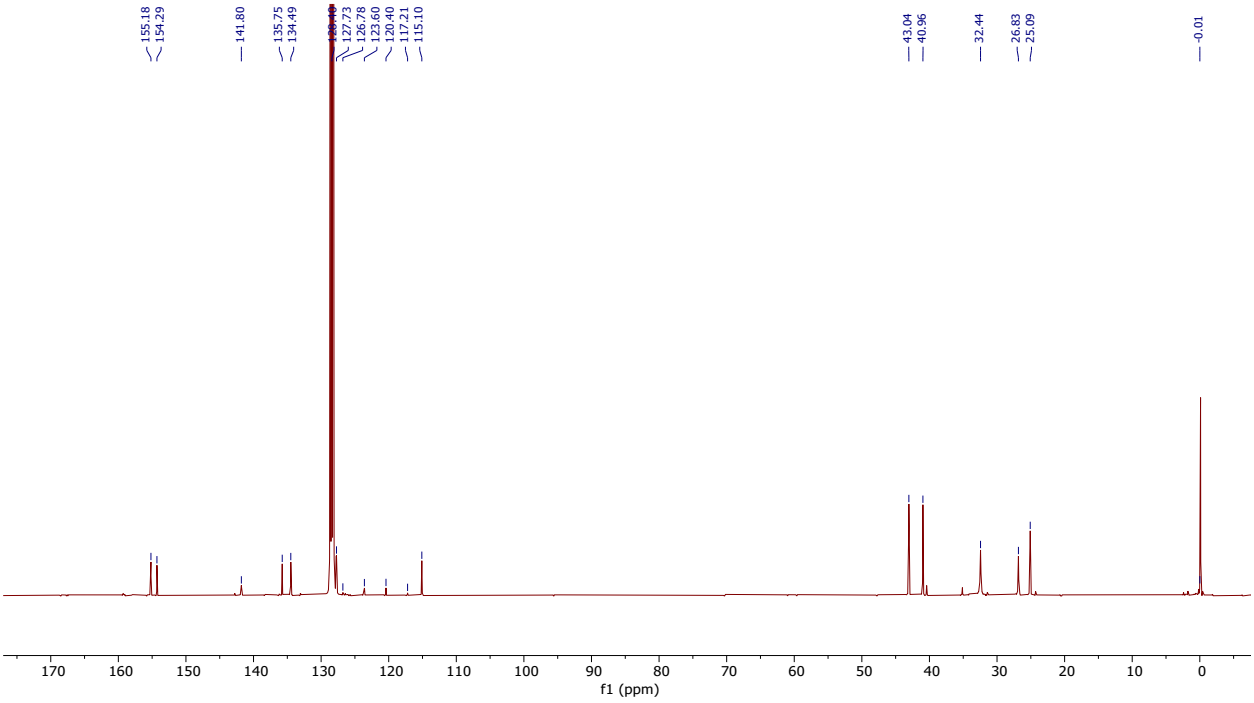

Figure S14. $^{13}C\{H\}$ NMR spectrum of **6** in C_6D_6 at room temperature.

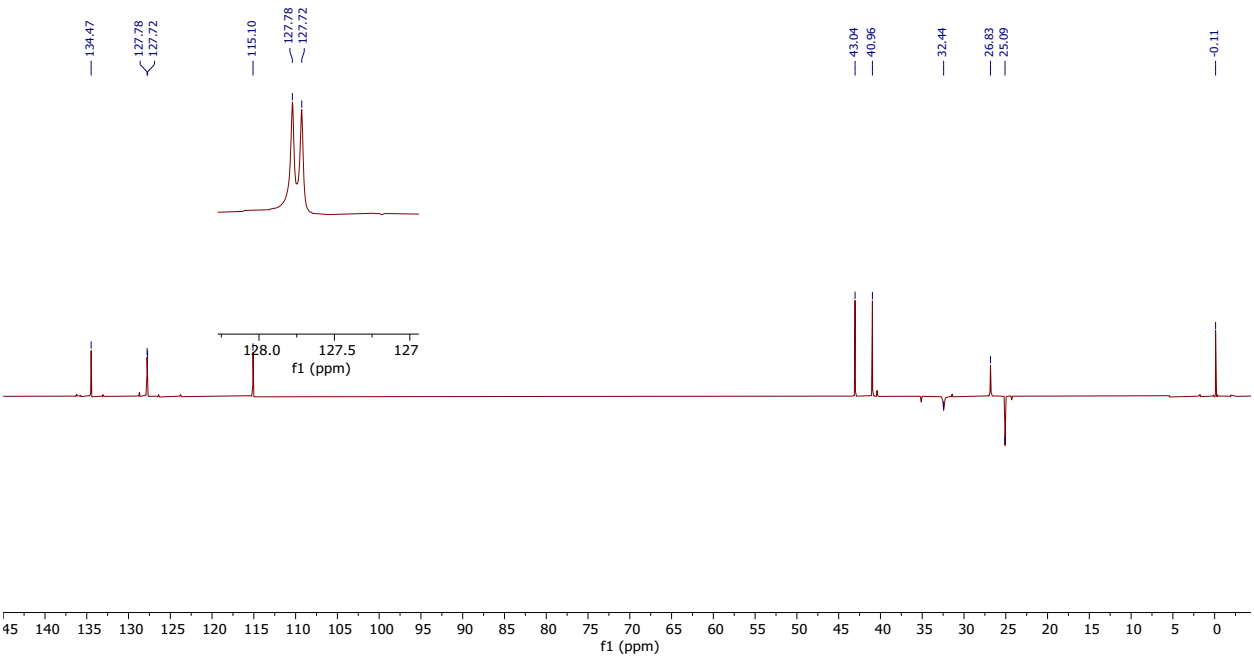

Figure S15. $^{13}C\{H\}$ (DEPT) NMR spectrum of **6** in C_6D_6 at room temperature.

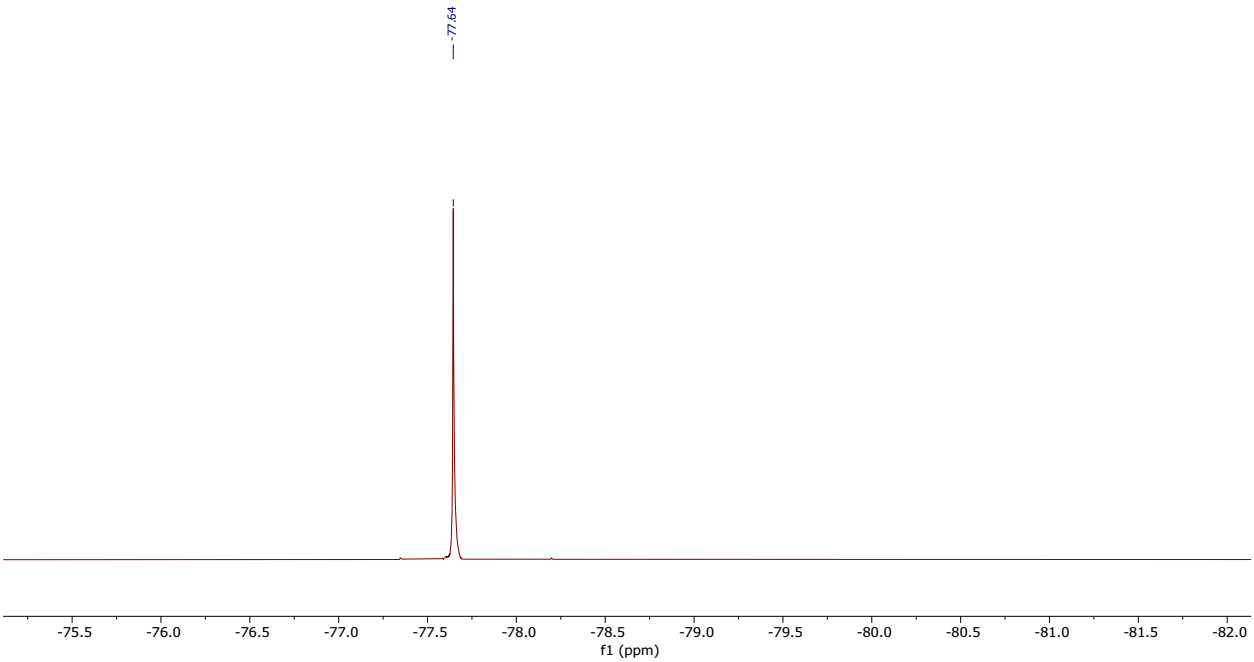

Figure S16. ^{19}F NMR spectrum of **6** in C_6D_6 at room temperature.

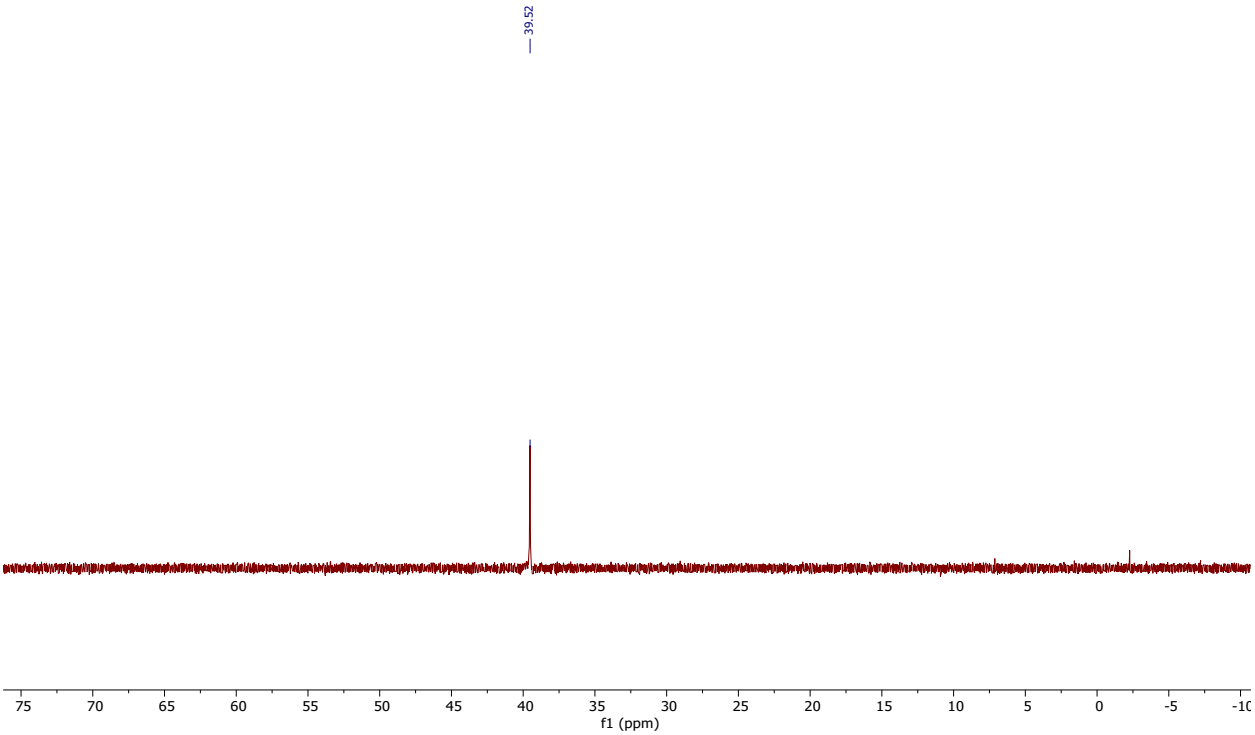

Figure S17. ^{29}Si NMR spectrum of **6** in C_6D_6 at room temperature.

2.5 Synthesis of **7**

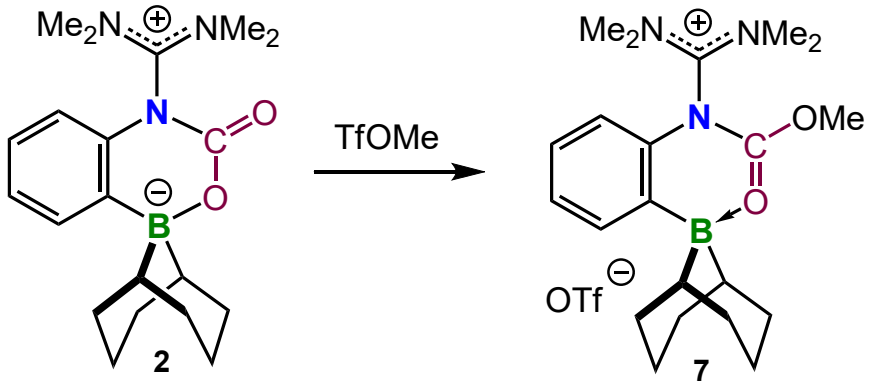

In the glove box, a 30 mL Schlenk flask was charged with **2** (100 mg, 0.28 mmol), MeOTf (50 mg, 0.30 mmol) and benzene (10 mL). After the reaction mixture was stirred for 2 hours at room temperature, all volatiles were removed under vacuum. The remaining solid residue was washed with hexanes (3 × 5 mL) and dried under vacuum to give **7** as a colorless solid. Yield 100 mg (70%). ^{1}H NMR [400 MHz, C_6D_6]: 8.02 (d, $^{3}J_{H\text{-}H}$ = 8 Hz, CH-aryl, 1 H), 7.30 (t, $^{3}J_{H\text{-}H}$ = 8 Hz, CH-aryl, 1 H), 7.16 (t, $^{3}J_{H\text{-}H}$ = 8 Hz, CH-aryl, 1 H), 6.69 (d, $^{3}J_{H\text{-}H}$ = 8 Hz, CH-aryl, 1 H), 3.82 (OMe), 3.20 (s, CH_3, 6 H), 2.84 (s, CH_3, 6 H), 1.95 -2.35 (m, CH_2-BBN, 12 H), 1.25 (s, CH-BBN, 2 H) ppm. ^{13}C{H} NMR [125 MHz, C_6D_6]: 157.0 (C=O), 154.4 (C=N), 142.0 (C-B), 135.6 (C-aryl), 134.4, 127.9, 127.4 (CH-aryl),122.5 (q, $^{1}J_{C\text{-}F}$ 258 Hz, CF_3), 115.3 (CH-aryl), 58.9 (OCH_3), 43.0, 41.0 (CH_3), 32.6 (CH_2), 26.6 (CH), 25.2 (CH_2) ppm. ^{19}F NMR [376.3 MHz, C_6D_6]: -77.9 ppm. The combustion analysis of the title compound gave unsatisfactory results.

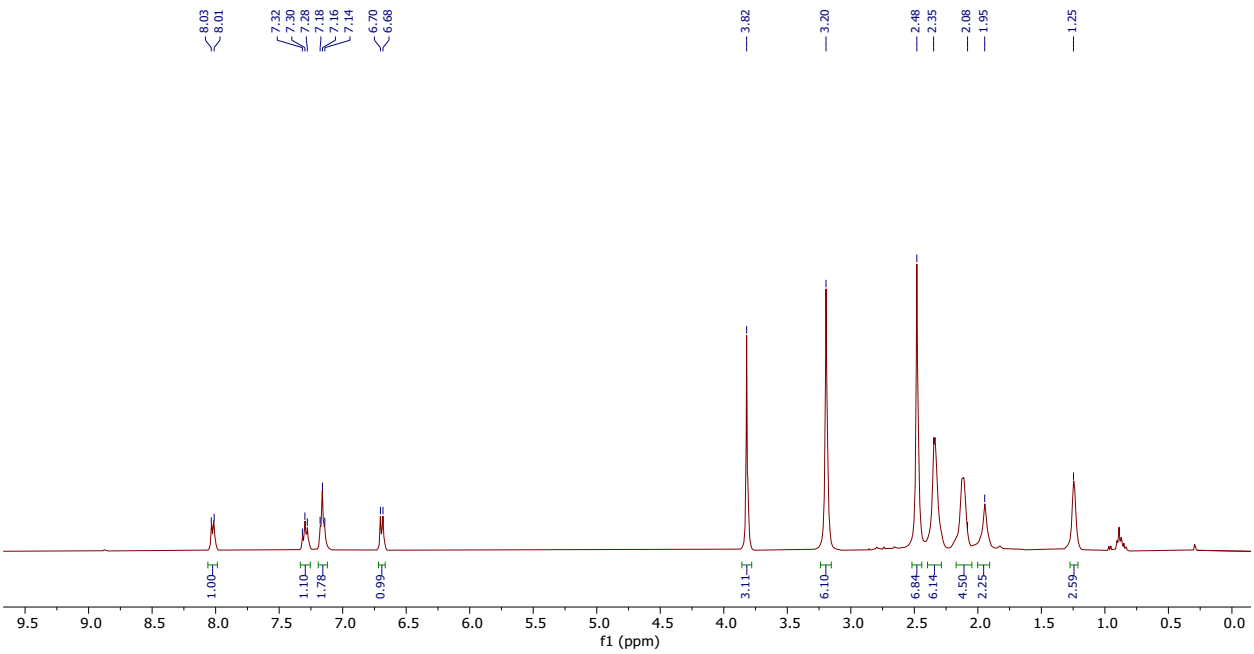

Figure S18. ^{1}H NMR spectrum of **7** in C_6D_6 at room temperature.

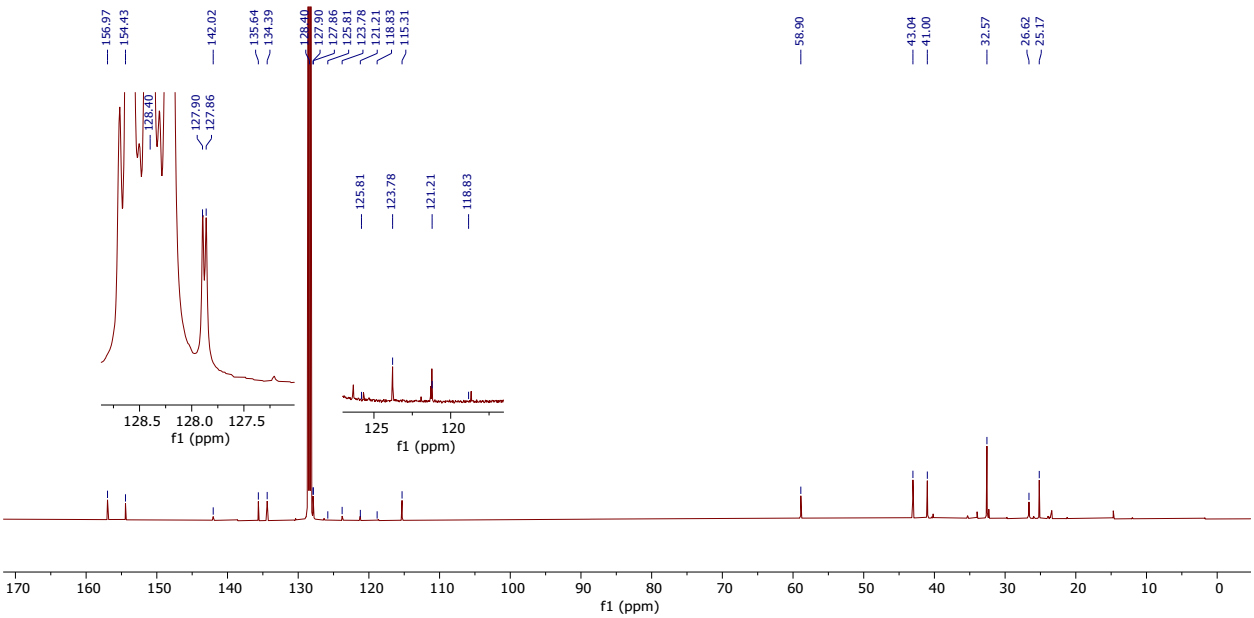

Figure S19. $^{13}C\{H\}$ NMR spectrum of **7** in C_6D_6 at room temperature.

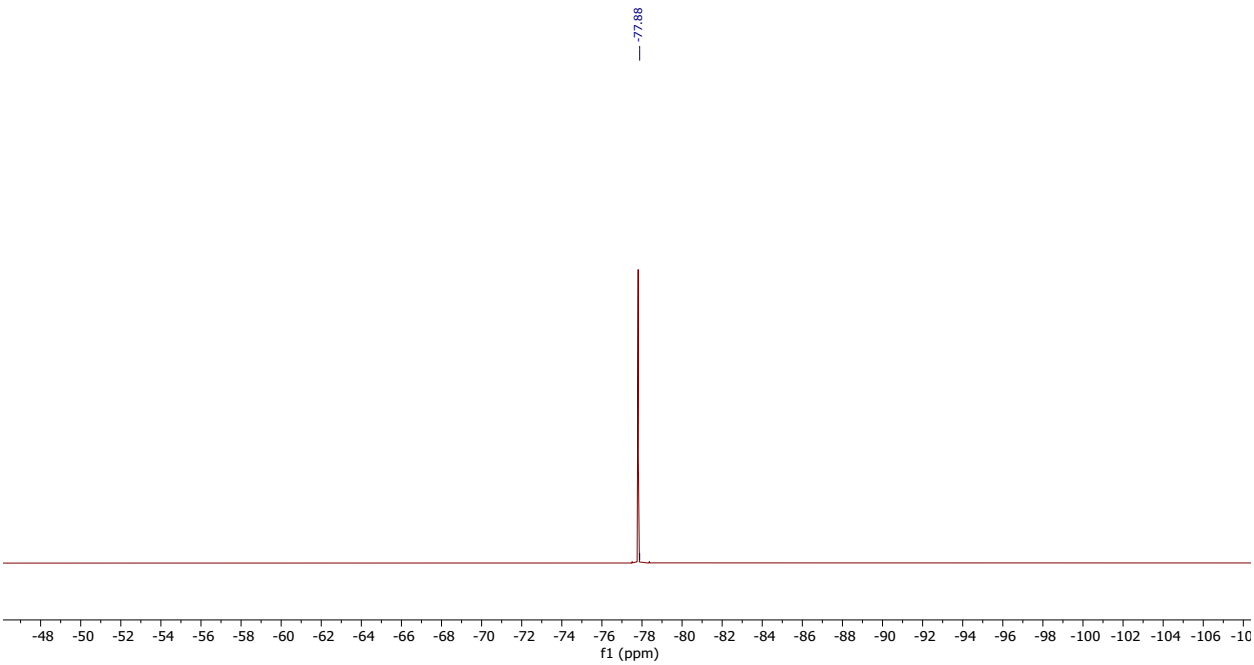

Figure S20. ^{19}F NMR spectrum of **7** in C_6D_6 at room temperature.

2.6 Formation of **8**

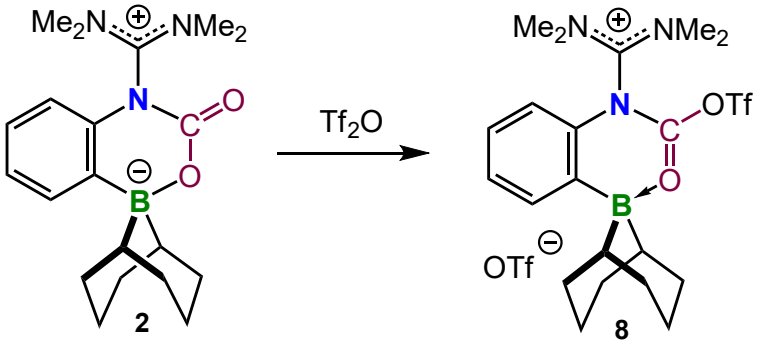

In the glove box, a J. Young NMR tube was charged with **2** (20 mg, 0.056 mmol), Tf_2O (15.8 mg, 0.056 mmol) and benzene (0.5 mL) and the reaction mixture was monitored by NMR spectroscopy. ^{1}H NMR [400 MHz, C_6D_6]: 7.74 (d, $^{3}J_{H-H}$ = 8 Hz, CH-aryl, 1 H), 7.45 (t, $^{3}J_{H-H}$ = 8 Hz, CH-aryl, 1 H), 7.07-7.10 (m, CH-aryl, 2 H), 3.29 (s, CH_3, 6 H), 2.48 (s, CH_3, 6 H), 1.70-2.22 (m, CH_2-BBN, 12 H), 1.44 (s, CH-BBN, 2 H) ppm. $^{13}C\{H\}$ NMR [125 MHz, C_6D_6]: 155.7 (C=O), 154.3 (C=N), 142.0 (C-B), 135.2 (C-aryl), 134.6, 127.9 (CH-aryl), 127.4 (CH-aryl), 120.8 (q, $^{1}J_{C-F}$ = 257 Hz, CF_3), 43.0, 40.8 (CH_3), 34.3, 32.5 (CH_2), 26.9, 26.7 (CH), 23.8, 23.1 (CH_2) ppm. ^{19}F NMR [376.3 MHz, C_6D_6]: -77.6 ppm.

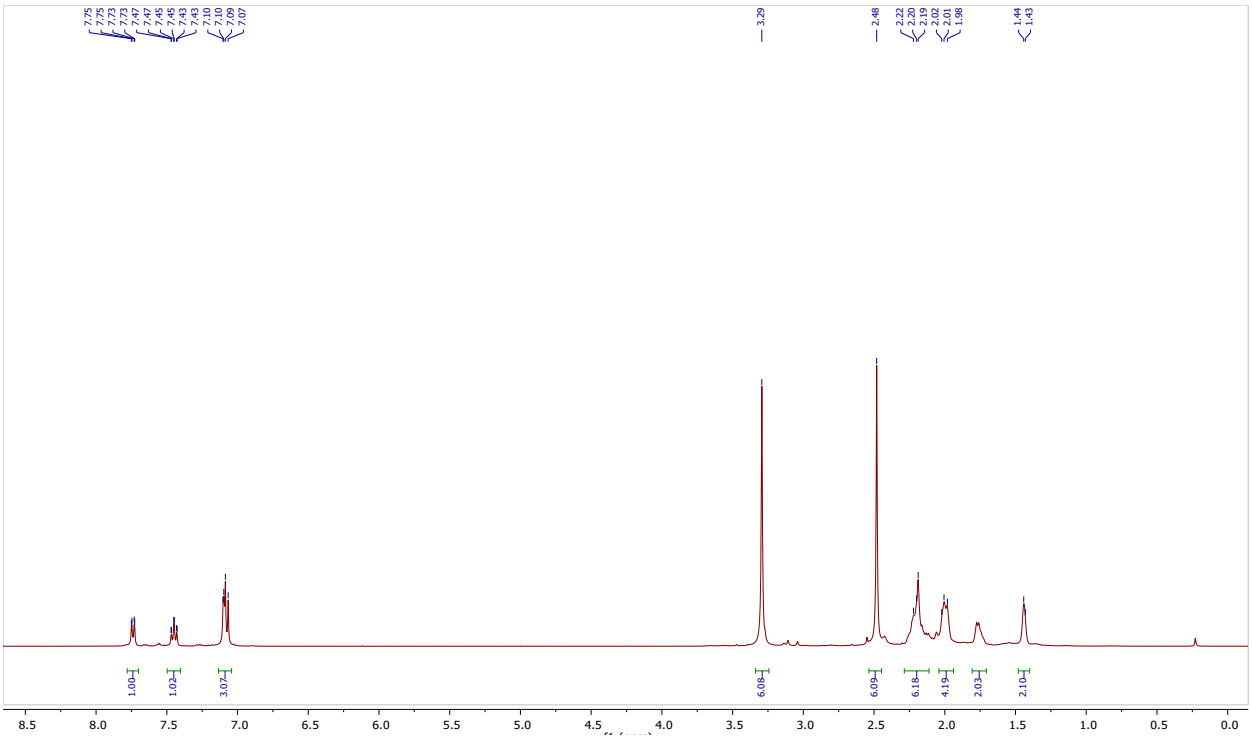

Figure S21. ^{1}H NMR spectrum of **8** in C_6D_6 at room temperature.

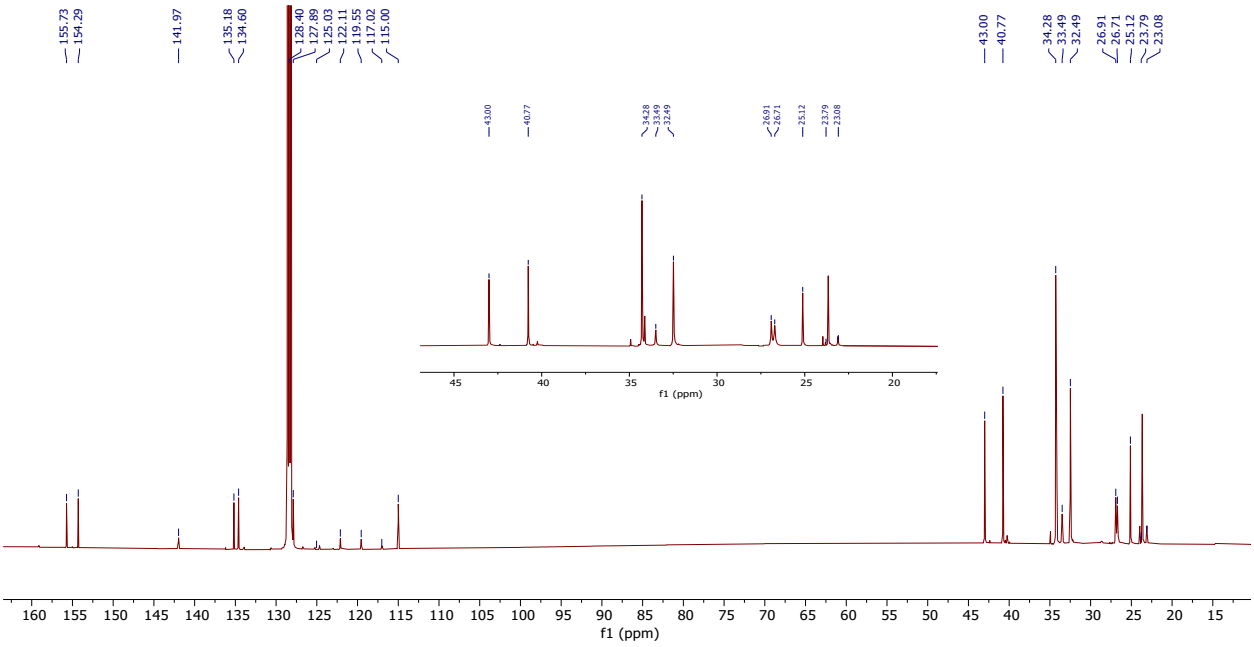

Figure S22. $^{13}C\{H\}$ NMR spectrum of **8** in C_6D_6 at room temperature.

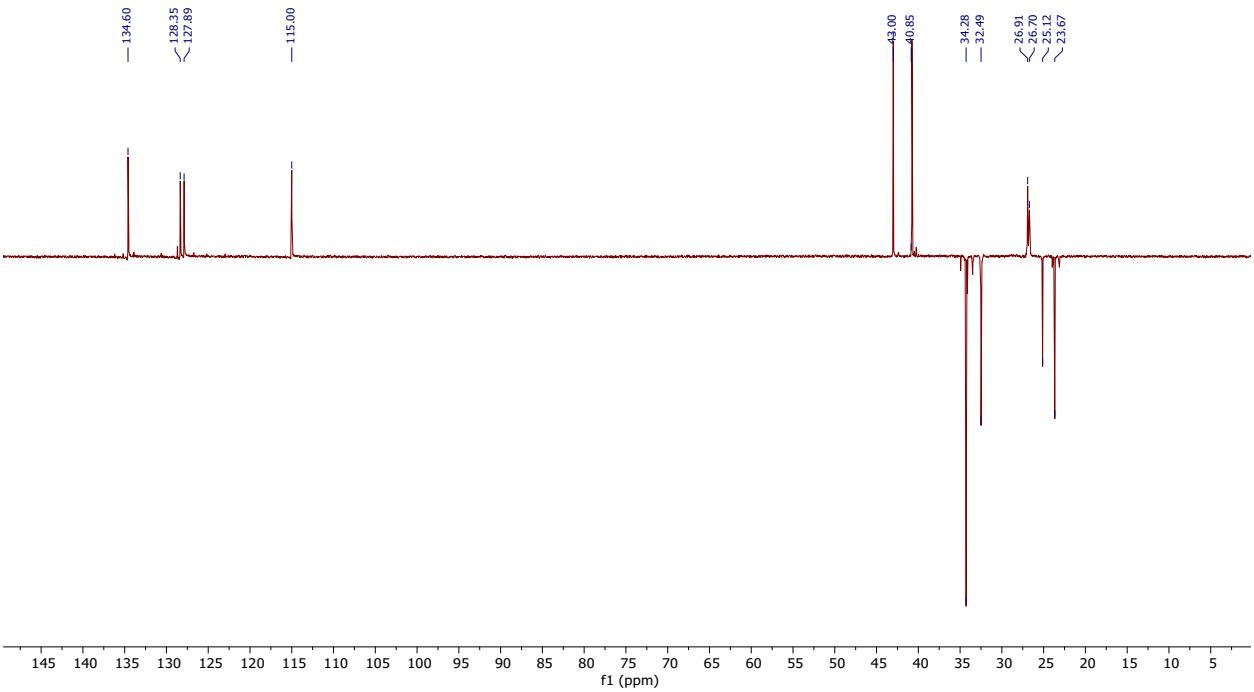

Figure S23. $^{13}C\{H\}$ (DEPT) NMR spectrum of **8** in C_6D_6 at room temperature.

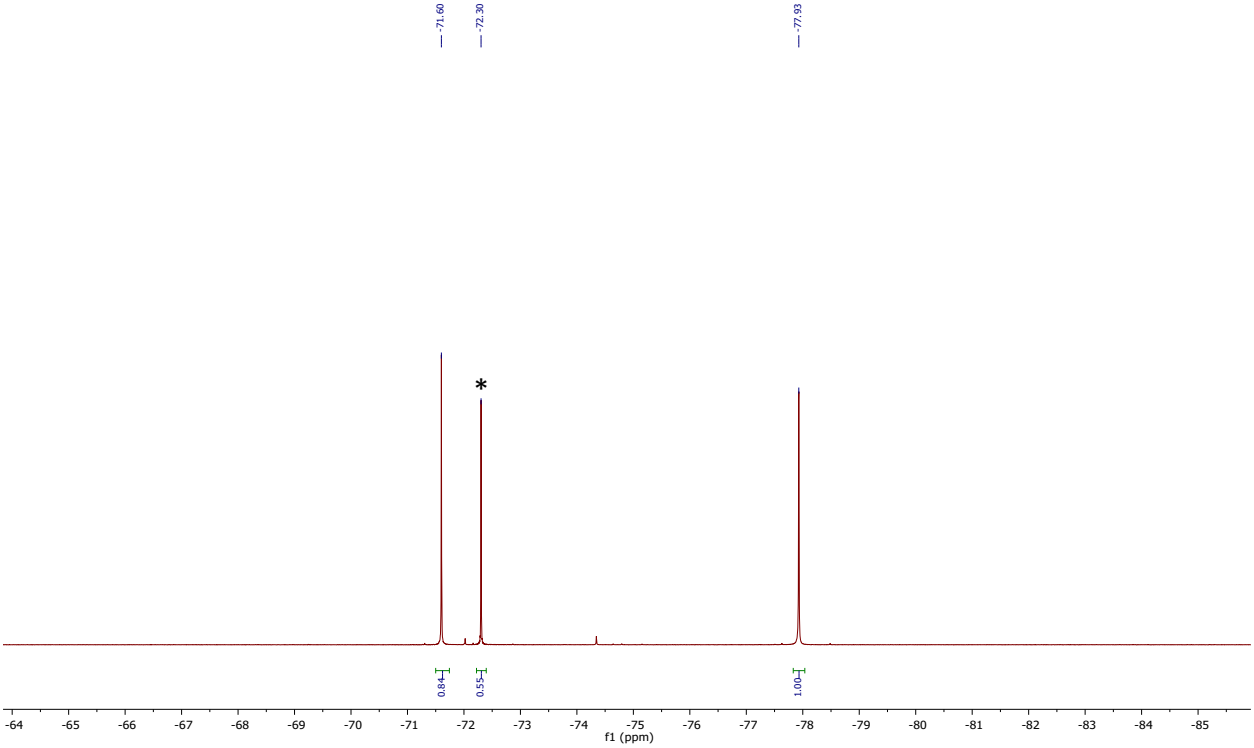

Figure S24. ^{19}F NMR spectrum of **8** in C_6D_6 at room temperature (residual Tf_2O labelled with asterisks).

2.7 Formation of **9** and **10**

In the glove box, a J. Young NMR tube was charged with **2** (20 mg, 0.056 mmol), Tf_2O (15.8 mg, 0.056 mmol) and CD_2Cl_2 (0.5 mL). After ca. 30 min, the reaction mixture was analyzed by NMR spectroscopy. Then, freshly distilled triethyl phosphine oxide (TPO) (7.5 mg, 0.056 mmol) was added and the reaction mixture analyzed by NMR spectroscopy (see below).

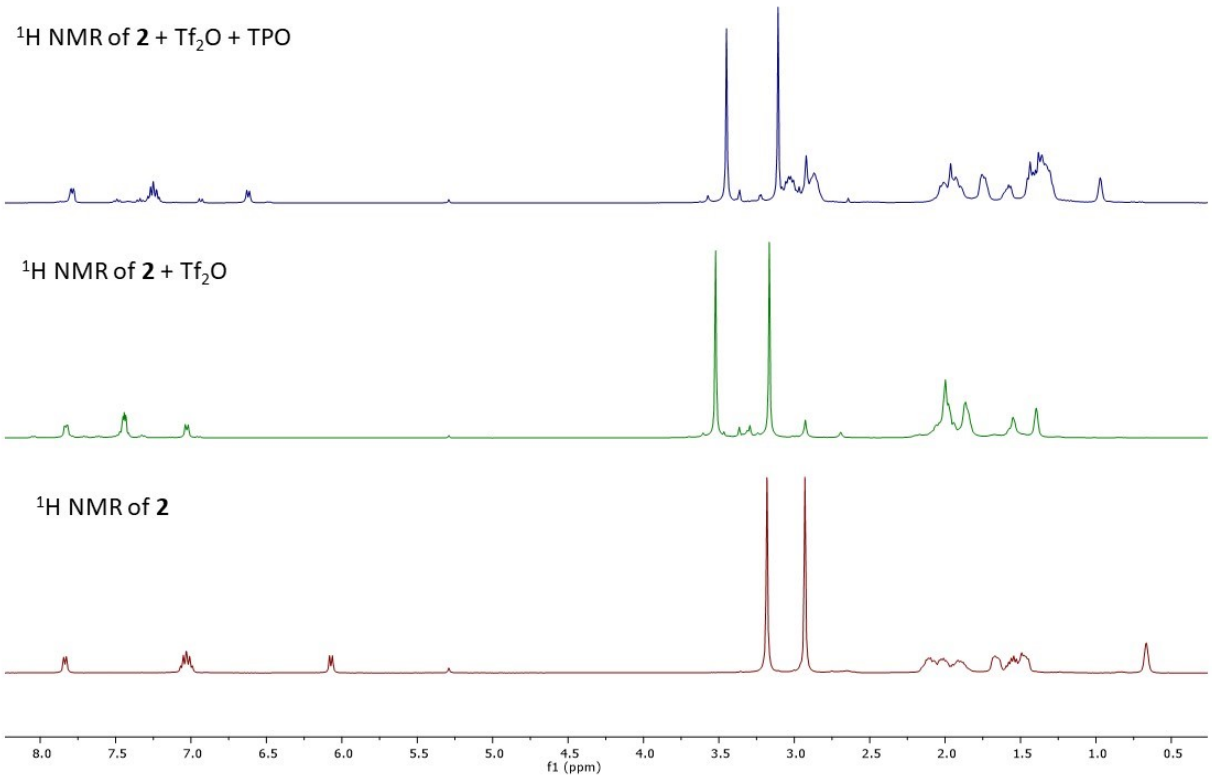

Figure S25. Stack plot of the ^{1}H NMR spectrum of the reaction of **2** with Tf_2O and TPO in CD_2Cl_2 at room temperature.

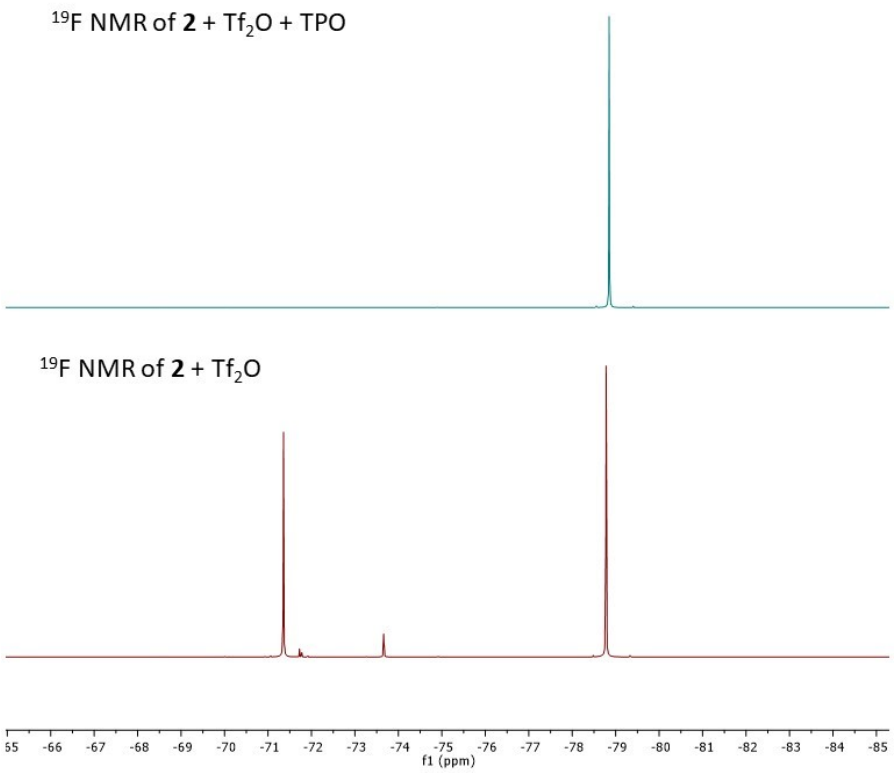

Figure S26. Stack plot of the ^{19}F NMR spectrum of the reaction of **2** with Tf_2O and TPO in CD_2Cl_2 at room temperature.

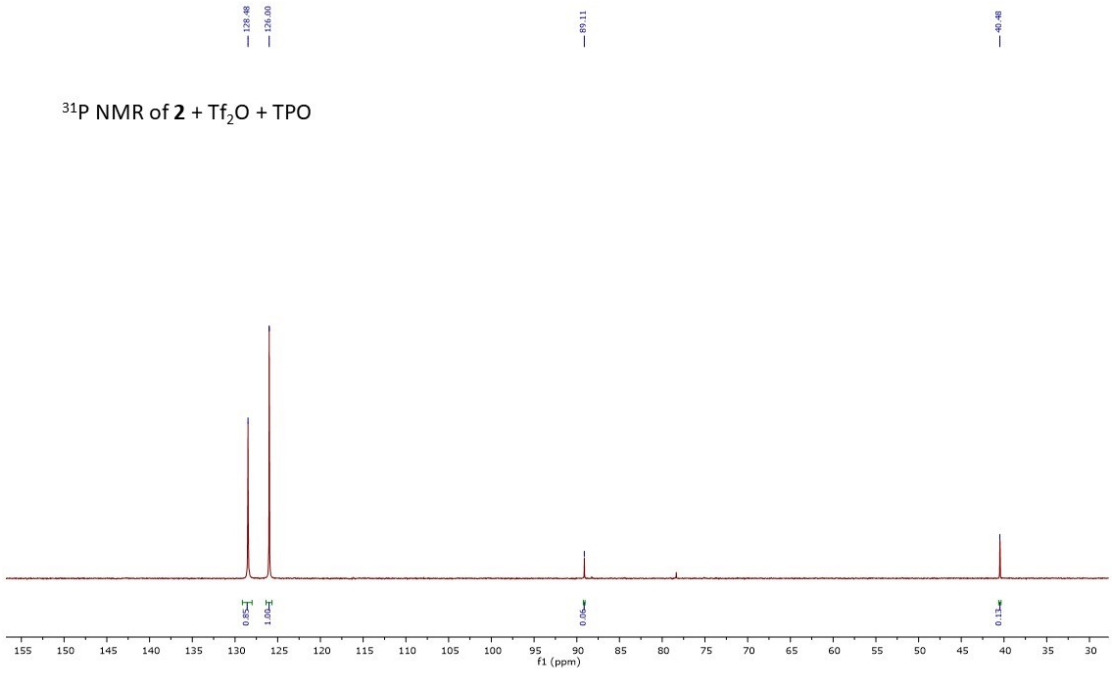

Figure S27. ^{31}P NMR spectrum of the reaction of **2** with Tf_2O and TPO in CD_2Cl_2 at room temperature.

2.8 Synthesis of **11**

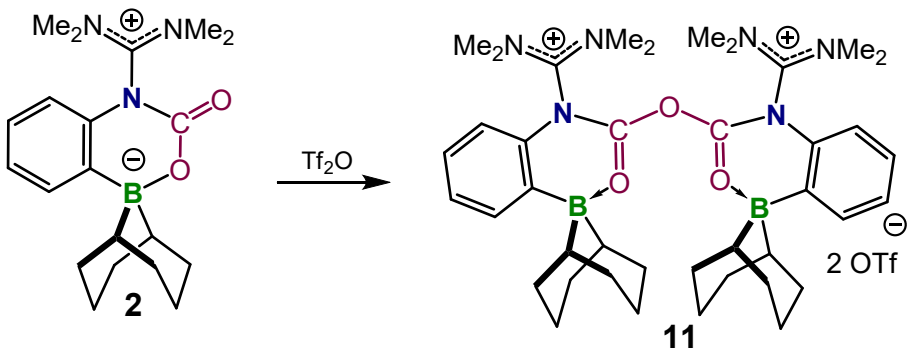

In the glove box, a solution of Tf_2O (19.85 mg, 0.07 mmol) in CD_2Cl_2 (0.5 mL) was added in one portion to a J. Young NMR tube charged with **2** (50 mg, 0.14 mmol). Then, the J. Young NMR tube with the resulting suspension was rotated for approximately 30 min until all **2** had disappeared. ^{1}H NMR and ^{19}F NMR spectra were taken to ensure complete consumption of **2**. Then, the solvent was removed under vacuum and the resulting precipitate was re-dissolved in benzene. After crude **11** precipitated within 5 days, the solvent was decanted. The remaining precipitate was washed twice with benzene and dried under vacuum to give pure **11** as a pale yellow solid (yield 50%). The solid-state structure of the crystalline material was analyzed by XRD and PXRD. IR (solid) $\tilde{\nu}_{(C=O)}$ = 1751 cm^{-1}; $\tilde{\nu}_{(C=N)}$ = 1664 cm^{-1}.

3. X-ray Crystallography

CCDC2127865 (**2**), CCDC2127866 (**3**), CCDC2127867 (**4**), CCDC2127868 (**5**), CCDC2127869 (**6**), CCDC2127870 (**8**), CCDC2127871 (**9**), CCDC2127872 (**11**), and CCDC2127873 (**12**) contain the supplementary crystallographic data for this paper.

These data can be obtained from the Cambridge Crystallographic Data Centre via http://www.ccdc.cam.ac.uk/data_request/cif, or from the Cambridge Crystallographic Data Centre, 12 Union Road, Cambridge CB2 1EZ, UK; fax: (+44) 1223-336-033; e-mail: deposit@ccdc.cam.ac.uk.

3.1. General Data Collection

All data for this manuscript were collected on a Rigaku XtaLAB Synergy-*i* Kappa diffractometer equipped with a PhotonJet-*i* X-ray source operated at 50 W (50kV, 1 mA) to generate Cu Kα radiation (λ = 1.54178 Å) and a HyPix-6000HE HPC detector. Crystals were transferred from the vial and placed on a glass slide in type NVH immersion oil by Cargille. A Zeiss Stemi 305 microscope was used to identify a suitable specimen for X-ray diffraction from a representative sample of the material. The crystal and a small amount of the oil were collected either on a MīTiGen cryoloop or a Hampton Research 20 micron nylon CryoLoop, depending on the crystal size, and transferred to the instrument where it was placed under a cold nitrogen stream (Oxford 700 series) maintained at 100K throughout the duration of the experiment. The sample was optically centered with the aid of a video camera to insure that no translations were observed as the crystal was rotated through all positions. A unit cell collection was then carried out. After it was determined that the unit cell was not present in the CCDC database a data collection strategy was calculated by *CrysAlis*^{Pro} [4]. The crystal was measured for size, morphology, and color. These values are reported in the combined CIF for each structure.

3.2. General Refinement Details

After data collection, the unit cell was re-determined using a subset of the full data collection. Intensity data were corrected for Lorentz, polarization, and background effects using the *CrysAlis*^{Pro} [4]. A numerical absorption correction was applied based on a Gaussian integration over a multifaceted crystal and followed by a semi-empirical correction for adsorption applied using the program *SCALE3 ABSPACK* [5]. The program *SHELXT* [6]. was used for the initial structure solution and *SHELXL* [7] was used for refinement of the structure. Both of these programs were utilized within the OLEX2 software [8]. Hydrogen atoms bound to carbon atoms were located in the difference Fourier map and were geometrically constrained using the appropriate AFIX commands.

3.3 Sample Specific Refinement Details

2 The structure was refined as an inversion twin during the final refinements with a resulting BASF value of 0.109.

3 In this structure the carbon atoms (C39 < C41) of the interstitial benzene molecule were modeled as disordered over two positions (A and B). To help maintain reasonable ADP values and C-C bond lengths, SIMU and free variable DFIX restraints were applied to the disordered sites.

5 Overall, the diffraction quality of the crystal was poor and due to the suspected loss of interstitial solvent molecules, there is slight disorder about the whole molecule. To help with maintaining reasonable ADP values the RIGU restraint was applied globally. Once the atom positions of the main molecule and one of the interstitial benzene molecules was determined, it was discovered that a substantial amount of the unit cell volume consisted of highly disordered and partial occupied benzene molecules. This electron density was treated as diffuse scattering using the SQUEEZE [9] routine within PLATO [10], which resulted in a total of four void spaces within the unit cell, each containing an electron count of 124.

8 In this structure the interstitial chlorobenzene molecule was positionally disordered about an inversion site. Atoms Cl1 and C23 < C28 had their site occupancies constrained to 0.5 to account for this disorder.

9 The triflate molecule (S1, O3 < O5, F1 < F3, and C27) in this structure was positionally disordered over two sites. Atoms S1, O5, C27, and F1 were split into parts A and B with refined occupancies of 0.94 and 0.06, respectively. To help maintain reasonable ADP values and bond lengths for the disordered sites, RIGU, SIMU, and free variable DFIX restraints were applied where necessary. The inconsistent reflections -9 -4 15 and -6 14 0 were omitted.

12 In this structure the hydrogen atom bound to N1 was allowed to free refine its position.

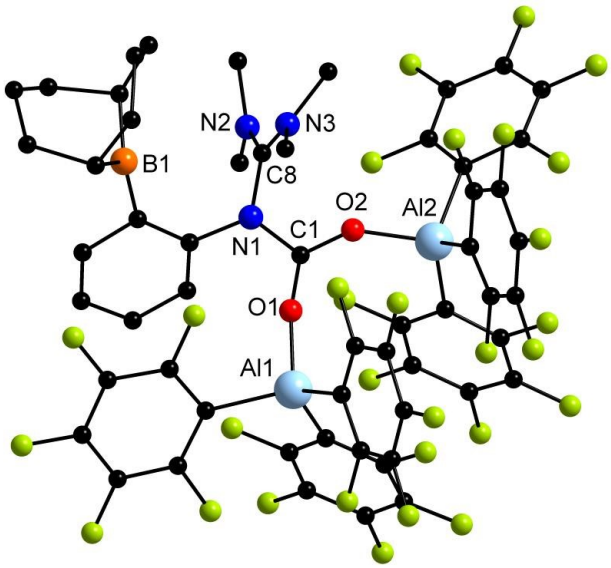

Figure S28. Solid-state structure of **5** (all H atoms are omitted for clarity); Selected distances [Å] and angles [°]: Al1 O1 1.804(4), Al2 O2 1.808(3), O1 C1 1.250(6), O2 C1 1.260(6), N1 C1 1.382(6), N1 C8 1.425(6), N2 C8 1.340(7), N3 C8 1.301(7), C1 O1 Al1 166.7(3), C1 O2 Al2 145.7(3), O1 C1 O2 125.1(4), O1 C1 N1 118.8(4), O2 C1 N1 116.1(4).

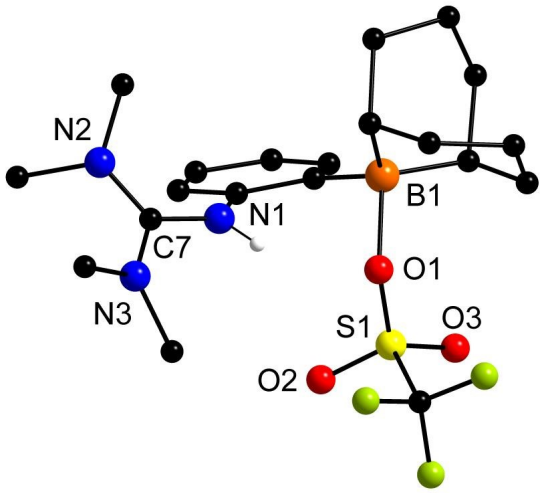

Figure S29. Solid-state structure of **12** (all H atoms bound to carbon are omitted for clarity); Selected distances [Å] and angles [°]: O1 B1 1.783(2), N1 C7 1.347(2), N2 C7 1.338(2), N3 C7 1.338(2).

3.4. Powder diffraction analysis of 11

A powder sample of **11** was obtained from grinding crystalline **11** in an agate mortar in the glove box. An oven-dried borosilicate glass capillary was charged with **11** and the diffraction data were collected on a Rigaku Ultima III powder diffractometer. The sample was packed into a thin-walled boron rich glass capillary with inside diameter of 0.7mm and wall thickness of 0.1mm (Charles Supper Company) to protect it from air. X-ray diffraction patterns were obtained by scanning a 2θ range of 3-50°, step size = 0.02°, and scan time of 5.0 min/degree. The X-ray source was Cu Kα radiation (λ =1.5418 Å) with an anode voltage of 40 kV and a current of 44 mA. The beam was then discriminated by Rigaku's Cross Beam parallel beam optics to create a monochromatic parallel beam. Diffraction intensities were recorded on a scintillation detector after being filtered through a Ge monochromator.

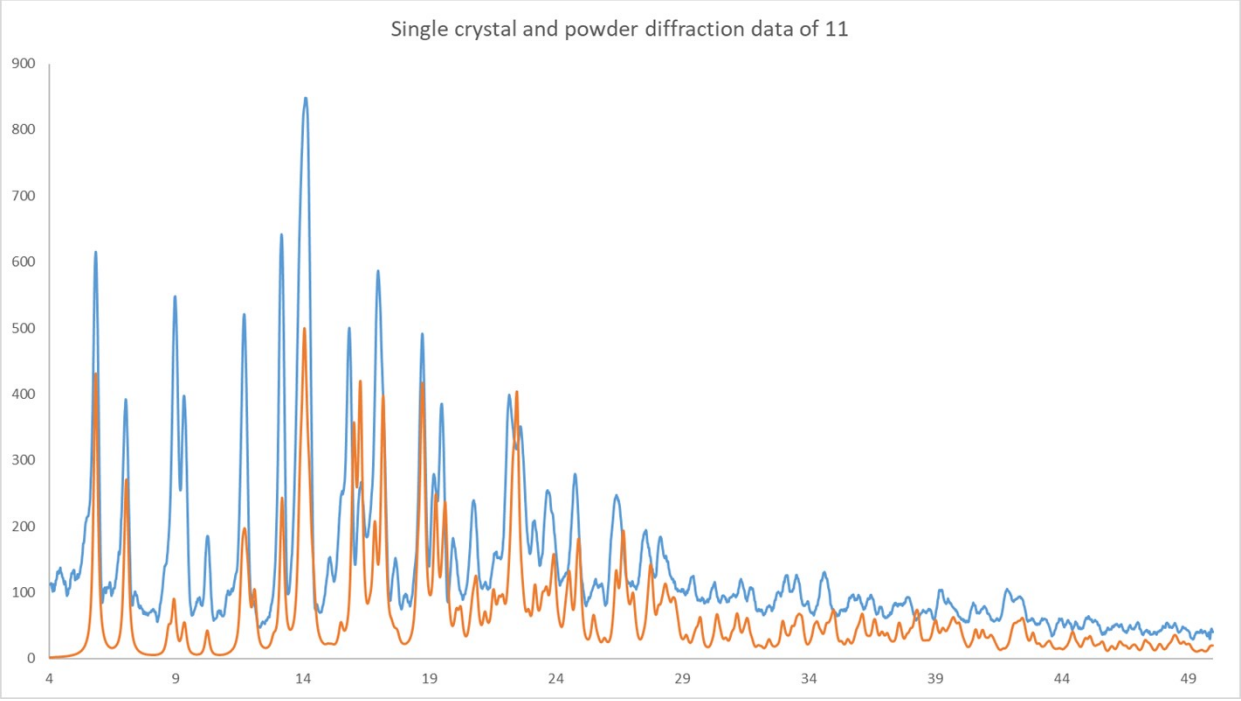

Figure S30. Stack plot of the single-crystal (shown in orange) and the powder diffraction data (shown in blue) of **11**.

4. Calculations

Theoretical calculations based in density functional theory (DFT) by means of the B3-LYP functional [11] and the triple-ζ valence polarization (TZVP) basis set were taken to the geometry, bond order, natural population analysis (NPA) [12] charge and harmonic frequencies calculations. The bond order of selected bonds was calculated by the spin-corrected Mayer bond order [13] in the natural atomic orbital (NAO) basis since it is reliable for molecular systems. The C=O and C=N stretching frequency values were corrected by a scale factor of 0.9654 [14]. Dispersion corrections were explicitly included in the calculations by using the Grimme empirical formalism D3 [15]. All calculations used the Gaussian 09 suite program [16].

Table S1. B3-LYP/TZVP Mayer bond order, atomic distances (Å) and atomic charges (e) of selected bonds in **11**.

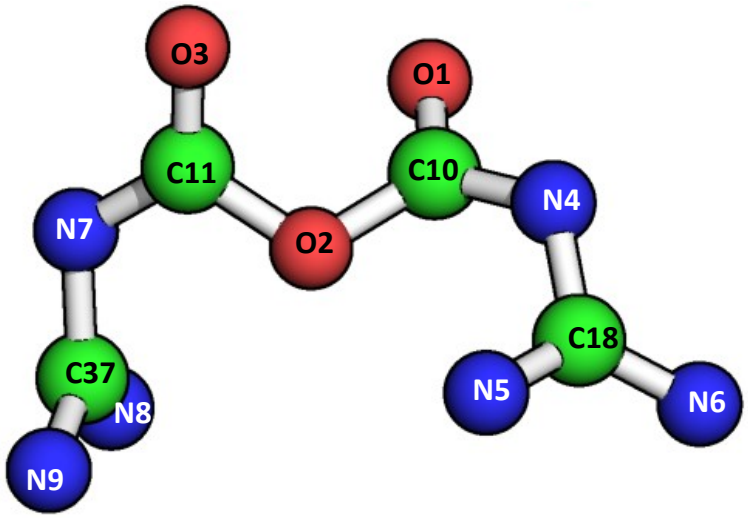

Bond	Bond order	Atomic distance	Atomic charge
C2-O1	1.721	1.220	0.9201/-0.4775
C2-O2	1.048	1.377	0.9149/-0.4699
C1-O2	1.067	1.373	0.9731/-0.4699
C1-O3	1.766	1.219	0.9731/-0.4857
C2-N4	1.300	1.339	0.9149/-0.4361
C12-N4	0.846	1.467	0.1247/-0.4361
C15-N4	1.055	1.433	0.6858/-0.4409
C15-N5	1.396	1.322	0.6858/-0.3224
C15-N6	1.530	1.318	0.6858/-0.3123
C1-N1	1.243	1.355	0.9412/-0.4559
C8-N1	0.983	1.417	0.6953/-0.4559
C8-N2	1.448	1.323	0.6953/-0.3165
C8-N3	1.467	1.322	0.6953/-0.3395

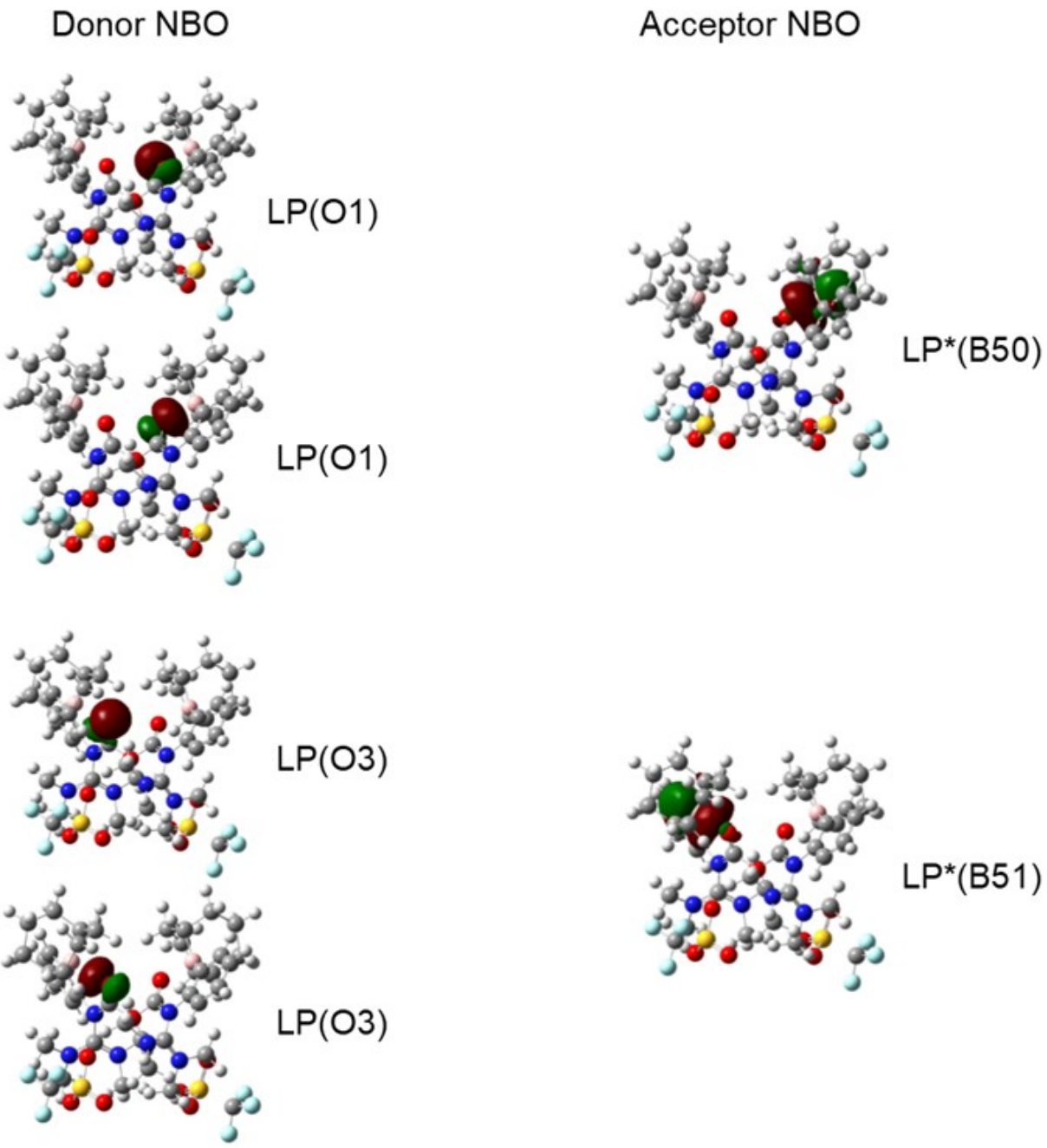

Figure S31. Donor filled lone pair (LP) and acceptor empty lone pair (LP*) natural bond orbitals of O1/O3 and B1/B2, respectively.

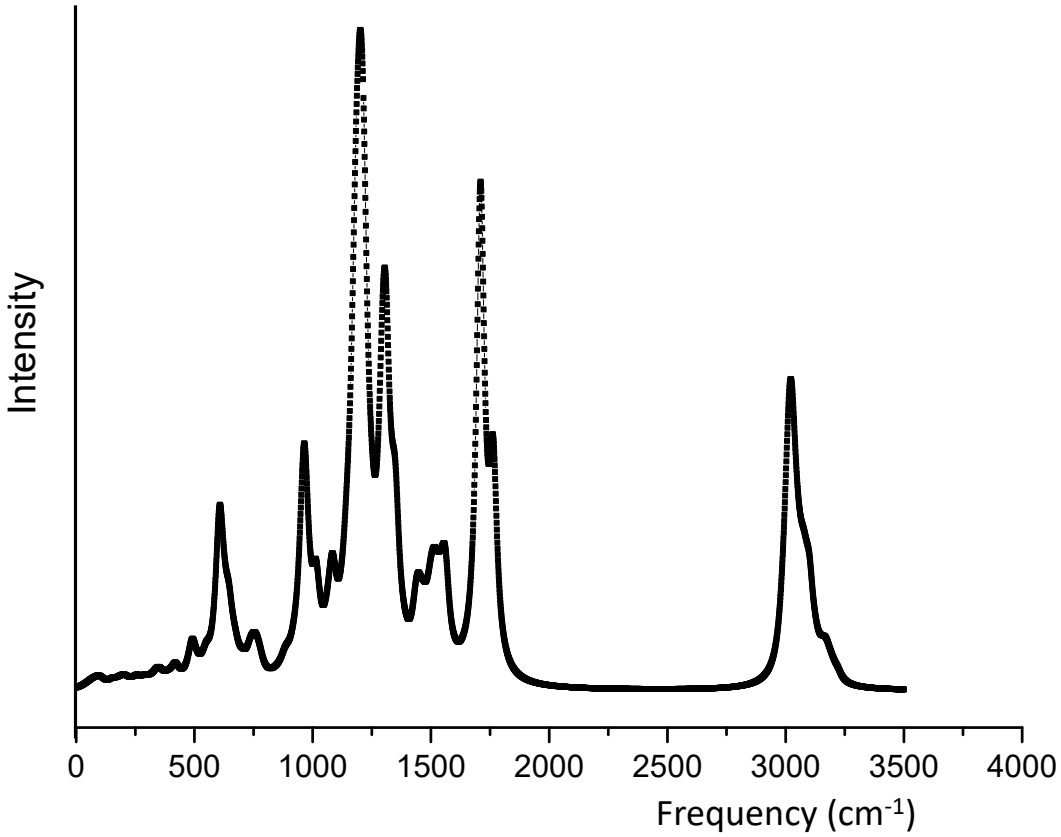

Figure S32. Calculated IR spectrum of **11** (B3-LYP/TZVP); C-N corrected frequency, 1646 cm^{-1}, C=O corrected frequency, 1703 cm^{-1}.

Optimized Cartesian Coordinates:

O	0.528905	2.101312	-0.068545
O	-0.016207	-0.065931	0.088195
O	-1.962004	0.963315	-0.262722
N	0.931452	0.998752	1.883129
N	0.021877	-0.588097	3.365737
N	2.099923	-0.971584	2.317343
N	-1.321131	-0.606457	-1.770674
N	-1.605895	-2.884845	-2.159983
N	0.554084	-2.031509	-1.853216

C	0.501786	1.094003	0.618746
C	-1.166487	0.119935	-0.637540
C	1.356904	2.202106	2.605235
C	1.569643	3.390061	1.892177
C	1.971474	4.482465	2.675605
C	2.166343	4.402447	4.048782
C	1.953304	3.199697	4.708232
C	1.541182	2.090912	3.982669
C	1.003416	-0.274625	2.537006
C	-1.310951	0.020533	3.281967
C	0.205831	-1.482558	4.517792
C	3.322748	-0.304425	1.803784
C	2.185159	-2.435142	2.495857
C	2.801406	3.284133	-0.555183
C	3.633399	4.578751	-0.402454
C	2.911395	5.863319	-0.853829
C	1.449838	5.994470	-0.372439
C	0.611235	4.689592	-0.401469
C	0.236566	4.272369	-1.844305
C	1.429396	3.833591	-2.719681
C	2.465094	2.923813	-2.022401
C	-2.188626	-0.066168	-2.820031
C	-3.199450	0.846314	-2.506366
C	-3.938238	1.312520	-3.605191
C	-3.690786	0.900569	-4.908300
C	-2.655014	0.011063	-5.172510
C	-1.888437	-0.466294	-4.120613
C	-0.759389	-1.898879	-1.914484
C	-1.198129	-4.123128	-2.824832
C	-3.033784	-2.810879	-1.831726
C	1.460117	-0.956600	-2.290301

C	1.204063	-3.225798	-1.285000
C	-3.725156	2.846578	-0.605010
C	-3.479522	3.025834	0.914149
C	-4.297945	2.082053	1.821685
C	-4.404270	0.618647	1.338605
C	-4.579949	0.424923	-0.182494
C	-5.969738	0.842793	-0.721797
C	-6.290910	2.341964	-0.583882
C	-5.151818	3.286551	-1.021645
B	1.447145	3.499118	0.287959
B	-3.502961	1.300705	-0.995164
S	-1.736256	-3.412424	1.406183
F	-3.717069	-2.694997	3.047179
F	-4.395559	-3.366725	1.091275
F	-3.717236	-4.815911	2.563330
O	-1.739550	-2.000118	0.909999
O	-1.623557	-4.436913	0.339418
O	-0.887474	-3.627750	2.605855
C	-3.505354	-3.595786	2.070405
S	4.620942	-2.026692	-1.174039
F	6.877961	-3.475481	-1.227502
F	7.033683	-1.632850	-0.083319
F	7.031669	-1.567832	-2.257186
O	4.173306	-2.691073	-2.424332
O	4.389886	-0.553334	-1.122506
O	4.228749	-2.736342	0.084616
C	6.513343	-2.187878	-1.190858
H	2.152281	5.427648	2.186894
H	2.487833	5.277114	4.600454
H	2.101936	3.116421	5.777057
H	1.371653	1.159199	4.502140

H	-1.439209	0.729656	4.101816
H	-2.047956	-0.775658	3.351144
H	-1.458450	0.526703	2.337729
H	-0.199662	-2.468842	4.303643
H	-0.332839	-1.036706	5.354250
H	1.258441	-1.545697	4.777028
H	3.502837	0.619884	2.347259
H	3.260380	-0.112296	0.735307
H	4.149991	-0.991470	1.945035
H	2.711933	-2.680115	3.418914
H	2.767675	-2.812733	1.657403
H	1.191608	-2.873987	2.495924
H	3.412748	2.463399	-0.158373
H	3.922439	4.677888	0.649589
H	4.571575	4.484602	-0.960138
H	3.478643	6.732357	-0.505330
H	2.939304	5.918981	-1.941598
H	0.948199	6.759792	-0.976015
H	1.443366	6.390374	0.646568
H	-0.324615	4.894692	0.132666
H	-0.492605	3.459329	-1.792049
H	-0.279205	5.100549	-2.344064
H	1.047008	3.317165	-3.606374
H	1.933065	4.721523	-3.102229
H	3.383470	2.903027	-2.618502
H	2.092887	1.896058	-2.032671
H	-4.738276	2.016410	-3.430732
H	-4.297356	1.283647	-5.719598
H	-2.432481	-0.298231	-6.185544
H	-1.063055	-1.139048	-4.318037
H	-0.243947	-3.991875	-3.326727

H	-1.959382	-4.361223	-3.568395
H	-1.135769	-4.932858	-2.098376
H	-3.203424	-2.076994	-1.055564
H	-3.332303	-3.782349	-1.447869
H	-3.603856	-2.555602	-2.726476
H	0.902880	-0.175322	-2.798894
H	2.198281	-1.390264	-2.962742
H	2.003721	-0.539693	-1.447609
H	0.462321	-3.868647	-0.821863
H	1.905726	-2.884283	-0.526931
H	1.786676	-3.748874	-2.041017
H	-3.019080	3.502933	-1.126600
H	-2.412930	2.884144	1.108698
H	-3.695696	4.061005	1.201690
H	-5.301453	2.491162	1.939699
H	-3.865564	2.093186	2.828589
H	-3.503045	0.071970	1.619791
H	-5.224306	0.127445	1.875226
H	-4.481504	-0.648438	-0.376245
H	-6.025808	0.558636	-1.778667
H	-6.750379	0.264322	-0.214993
H	-7.188107	2.570380	-1.167751
H	-6.558407	2.551538	0.451466
H	-5.352366	4.289570	-0.627827
H	-5.179522	3.397173	-2.108764

5. References

[1] C. Manankandayalage, D. K. Unruh, C. Krempner, *Chem. Eur. J.* **2021**, *27*, 6263-6273.

[2] Feng, S.; Roof, G. R.; Chen, E. Y. X., *Organometallics*, **2002**, *21*, 832–839.

[3] Lancaster, S., *ChemSpider Synthetic Pages*, **2003**, 215.

[4] CrysAlis^{Pro} **2018** Oxford Diffraction Ltd.

[5] SCALE3 ABSPACK **2005** Oxford Diffraction Ltd.

[6] Sheldrick, G. M. *Acta Crystallogr*. **2015**, *C71*, 3-8.

[7] Sheldrick, G. M. *Acta Crystallogr*. **2015**, *A71*, 3-8.

[8] Dolomanov, O. V.; Bourhis, L. J.; Gildea, R. J.; Howard, J. A. K.; Puschmann. H., *J. Appl. Cryst*. **2009**, *42*, 339-341.

[9] Spek, A. L., *Acta Cryst.* **2009**, *D65*, 148-155.

[10] Spek, A. L., *Acta Cryst.* **2015**, *C71*, 9-18.

[11] A. D. Becke, J. Chem. Phys. 1993, 98, 5648−5652.

[12] A. E. Reed, R.B. Weinstock, F. Weinhold, J. Chem. Phys. Vol. 83, (1985),735-746.

[13] I. Mayer, Int. J. Quant. Chem. Vol. 29, (1986), 73-84.

[14] M. L. Laury, M. J. Carlson, and A. K. Wilson, J. Comp. Chem. 2012,33, 2380- 2387.

[15] S. Grimme, J. Antony, S. Ehrlich, and H. Krieg, J. Chem. Phys. 2010, 132, 154104.

[16] Gaussian 09, Revision A.02, M. J. Frisch, G. W. Trucks, H. B. Schlegel, G. E. Scuseria, M. A. Robb, J. R. Cheeseman, G. Scalmani, V. Barone, G. A. Petersson, H. Nakatsuji, X. Li, M. Caricato, A. Marenich, J. Bloino, B. G. Janesko, R. Gomperts, B. Mennucci, H. P. Hratchian, J. V. Ortiz, A. F. Izmaylov, J. L. Sonnenberg, D. Williams-Young, F. Ding, F. Lipparini, F. Egidi, J. Goings, B. Peng, A. Petrone, T. Henderson, D. Ranasinghe, V. G. Zakrzewski, J. Gao, N. Rega, G. Zheng, W. Liang, M. Hada, M. Ehara, K. Toyota, R. Fukuda, J. Hasegawa, M. Ishida, T. Nakajima, Y. Honda, O. Kitao, H. Nakai, T. Vreven, K. Throssell, J. A. Montgomery, Jr., J. E. Peralta, F. Ogliaro, M. Bearpark, J. J. Heyd, E. Brothers, K. N. Kudin, V. N. Staroverov, T. Keith, R. Kobayashi, J. Normand, K. Raghavachari, A. Rendell, J. C. Burant, S. S. Iyengar, J. Tomasi, M. Cossi, J. M. Millam, M. Klene, C. Adamo, R. Cammi, J. W. Ochterski, R. L. Martin, K. Morokuma, O. Farkas, J. B. Foresman, and D. J. Fox, Gaussian, Inc., Wallingford CT, 2016.